ACI 349.1R-07

Reinforced Concrete Design for Thermal Effects on Nuclear Power Plant Structures

Reported by ACI Committee 349

American Concrete Institute®

First printing
June 2007

American Concrete Institute®
Advancing concrete knowledge

Reinforced Concrete Design for Thermal Effects on Nuclear Power Plant Structures

The technical committees responsible for ACI committee reports and standards strive to avoid ambiguities, omissions, and errors in these documents. In spite of these efforts, the users of ACI documents occasionally find information or requirements that may be subject to more than one interpretation or may be incomplete or incorrect. Users who have suggestions for the improvement of ACI documents are requested to contact ACI. Proper use of this document includes periodically checking for errata at **www.concrete.org/committees/errata.asp** for the most up-to-date revisions.

ACI committee documents are intended for the use of individuals who are competent to evaluate the significance and limitations of its content and recommendations and who will accept responsibility for the application of the material it contains. Individuals who use this publication in any way assume all risk and accept total responsibility for the application and use of this information.

All information in this publication is provided "as is" without warranty of any kind, either express or implied, including but not limited to, the implied warranties of merchantability, fitness for a particular purpose or non-infringement.

ACI and its members disclaim liability for damages of any kind, including any special, indirect, incidental, or consequential damages, including without limitation, lost revenues or lost profits, which may result from the use of this publication.

It is the responsibility of the user of this document to establish health and safety practices appropriate to the specific circumstances involved with its use. ACI does not make any representations with regard to health and safety issues and the use of this document. The user must determine the applicability of all regulatory limitations before applying the document and must comply with all applicable laws and regulations, including but not limited to, United States Occupational Safety and Health Administration (OSHA) health and safety standards.

Order information: ACI documents are available in print, by download, on CD-ROM, through electronic subscription, or reprint and may be obtained by contacting ACI.

Most ACI standards and committee reports are gathered together in the annually revised *ACI Manual of Concrete Practice* (MCP).

American Concrete Institute
38800 Country Club Drive
Farmington Hills, MI 48331
U.S.A.
Phone: 248-848-3700
Fax: 248-848-3701

www.concrete.org

ISBN 978-0-87031-246-05

Reinforced Concrete Design for Thermal Effects on Nuclear Power Plant Structures

Reported by ACI Committee 349

Ronald J. Janowiak*
Chair

Omesh B. Abhat
Adeola K. Adediran
Hansraj G. Ashar
Ranjit L. Bandyopadhyay
Peter J. Carrato
Ronald A. Cook
Rolf Eligenhausen
Werner A. F. Fuchs
Branko Galunic
Partha S. Ghosal*
Herman L. Graves, III
Orhan Gurbuz*
James A. Hammell
Gunnar A. Harstead*
Christopher Heinz
Charles J. Hookham*
Scott A. Jensen*
Jagadish R. Joshi
Richard E. Klingner
Nam-Ho Lee
Dan J. Naus*
Dragos A. Nuta
Richard S. Orr*
Bozidar Stojadinovic
Barendra K. Talukdar
Donald T. Ward
Andrew S. Whittaker
Albert Y. C. Wong
Charles A. Zalesiak*

*Committee 349 members who were major contributors to the development of this report.

This report presents a design-oriented approach for considering thermal effect on reinforced concrete structures. Although the approach is intended to conform to the general provisions of Appendix E of ACI 349, it is not restricted to nuclear power plant structures. The general behavior of structures under thermal effects is discussed together with the significant issues to consider in reinforcement design. Two types of structures—frames and axisymmetric shells—are addressed. For frame structures, a rationale is described for determining the extent of component cracking that can be assumed for purposes of obtaining the cracked structure thermal forces and moments. Stiffness coefficients and carryover factors are presented in graphical form as a function of the extent of component cracking along its length and the reinforcement ratio. Fixed-end thermal moments for cracked components are expressed in terms of these factors for: 1) a temperature gradient across the depth of the component; and 2) end displacements due to a uniform temperature change along the axes of adjacent components. For the axisymmetric shells, normalized cracked section thermal moments are presented in graphical form. These moments are normalized with respect to the cross-sectional dimensions and the temperature gradient across the section. The normalized moments are presented as a function of the internal axial forces and moments acting on the section and the reinforcement ratio. Use of the graphical information is illustrated by examples.

Keywords: cracking (fracturing); frames; nuclear power plants; shells; structural analysis; structural design; temperature; thermal effect; thermal gradient; thermal properties.

CONTENTS

ACI 349.1R-07 supersedes ACI 349.1R-91 and was adopted and published May 2007.

CHAPTER 1—INTRODUCTION

1.1—General

ACI 349, Appendix E, provides general considerations in designing reinforced concrete structures for nuclear power plants subject to thermal effects. Thermal effects are defined to be the exposure of a structure or component thereof to varying temperature at its surface or temperature gradient through its cross section; the resulting response of the exposed structure is a function of its age and moisture content, temperature extreme(s), duration of exposure, and degree of restraint. The terms "force," "moment," and "stress" apply and are used in this report where a structure is restrained against thermally induced movements. Further treatment of these forces, moments, and stresses are contained in this report as a function of type of structure.

The Commentary to Appendix E, Section RE.1.2, of ACI 349-06 (ACI Committee 349 2006) instructs the designer to consider the following:

1. Linear thermal strain causes stress only under conditions of restraint, and a portion of such stress may be self-relieving. Mechanisms for relief are: cracking, yielding, relaxation, creep, and other time-dependent deformations; and

2. Accident temperature transients may be of such short duration that the resulting temperature distributions and corresponding stress changes are not significant. Therefore, these temperature transients may not adversely affect the safe shutdown capacity of the plant.

The Commentary to Appendix E, Section RE.3.3, of ACI 349-06 addresses three approaches that consider thermal effects in conjunction with all mechanical loads acting on the structure. One approach is to consider the structure uncracked under the mechanical loads and cracked under the thermal effects. The results of two such analyses are then combined.

The Commentary to Appendix E also contains a method of treating temperature distributions across a cracked section. In this method, an equivalent linear temperature distribution is obtained from the temperature distribution, which can generally be nonlinear. The linear temperature distribution is then separated into a pure gradient ΔT and into the difference between the mean and base (stress-free) temperatures $T_m - T_b$.

This report discusses approaches for making an assessment of thermal effects that are consistent with the aforementioned provisions. The goal is to present a designer-oriented approach for determining the reduced thermal moments that result from cracking of the concrete structure. Thermal effects should be considered in design for serviceability. The report discusses conditions under which it can be shown that the thermal effects do not adversely affect the safe shutdown capacity of the plant. Behavior and general guidance is addressed in Chapter 1. Chapter 2 addresses notation and definitions. Chapter 3 addresses frame structures, and Chapter 4 deals with axisymmetric structures. For frame structures, general criteria are given in Sections 3.2 (Section cracking) and 3.3 (Component cracking). The criteria are then formulated for the moment distribution method of structural analysis in Section 3.4. Cracked component fixed-end moments, stiffness coefficients, and carryover factors are derived and presented in graphical form. For axisymmetric structures, an approach is described for regions away from discontinuities, and graphs of cracked section thermal moments are presented.

This report is intended to propose simplifications that may be used for structural assessments. It will permit exclusion of thermal cases with small effect and a reduction of thermal effects for a large class of thermal cases without resorting to sophisticated and complex solutions (Appendix E, 349-06). Also, as a result of the report discussion, the design examples, and graphical presentation of cracked section thermal moments, it is hoped that a designer will better understand how thermal effects are influenced by the presence of other loads and the resulting concrete response, primarily in the form of cracking, although reinforcement yielding, concrete creep, nonlinear concrete stress-strain, and shrinkage are also very significant in mitigating thermal effects in concrete structures.

1.2—Thermal effects and structural responses

Thermal effects cause expansion or contraction of the components in a structural system. If the components are restrained, which is usually the case, stresses are induced. It is sufficient to note that there are three types of thermal effects:

1. Bulk temperature change. In this case, the entire structural component (or segments of the component) is subject to a uniform temperature change;

2. Thermal gradient. A temperature crossfall or thermal gradient is caused by different thermal conditions on two faces of a structure, such as two sides of a wall or the top and bottom of a beam; and

3. Local thermal exposure. Elevated temperature at a local surface caused by an external source such as operating equipment or piping or an abnormal event such as a fire.

Thermal effects will result in different states of stress and strain in structural components as a function of restraints. The analysis for thermal effects must distinguish between different types of thermal effects and properly characterize the structural response accordingly (for example, the degree of fixity of end and boundary restraints, component stiffness, influence of cracking, and concrete and reinforcing steel strain).

Thermal effects can arise from many sources including, but not limited to, process fluid transport; proximity to hot gasses, steam, or water passage (for example, reactor vessel or steam piping from reactor building to turbine); fire; or gradients formed when opposing faces of a structure are

exposed to differing temperatures (for example, spent fuel pool) or cyclic gradients from plant startup and shutdown. Temperature change is manifested under one or more of the following transfer mechanisms:

1. Radiation. The electromagnetic transfer of heat from a higher temperature source to a lower temperature surface of the concrete structure, such as from a radiator heating a room and the surrounding wall and floor structures;

2. Convection. The transfer of heat usually by the movement of a liquid or gas across a surface, such as from environmental temperature changes in the air next to a concrete structure; and

3. Conduction. The transfer of heat through a solid, such as from a steam pipeline into the surrounding concrete at a penetration.

There are many instances where all three mechanisms are present, such as in the case of a fire acting on a structure. Radiation and convection from the flame itself transfers heat to the impinged structure. The surface of the flame radiates heat, which is absorbed by the concrete and reinforcing steel; finally, heat is transferred away from the flame-impinged area by means of conduction through the structure. The structure will also lose heat by means of convection and radiation.

Response of a structure to thermal effects depends on the nature of the temperature distribution, end constraints, material properties, and mechanical loads. A proper thermal stress analysis must take these parameters into account.

Stresses in the concrete and reinforcement occur due to restraint of thermal movement and these stresses are generally self-relieving. These thermal stresses are generally small, as most thermal exposures are within prescribed ACI 349 temperature limits. Furthermore, internally generated stresses are complex to analyze given the size and geometry of safety-related concrete structures. As such, structural analyses using manual calculations with simplifying, conservative assumptions (for example, concrete is cracked) are typically considered to be appropriate. Computer-based analysis tools may also be used to determine the effects of thermal exposure and structure response as illustrated in the following paragraphs. It should be noted that a thorough and complete computer-based thermal analysis is much more complicated than a structural analysis of mechanical loads. The difficulty of defining important parameters would also make such computer thermal analyses controversial because differences in parameter ranges may produce significant differences in analytical results. Finally, it is known that ambient thermal effects, in all but very unusual situations (for example major fire events), will have little effect on the ultimate strength of a concrete structure.

1.3—General guidelines

Stresses resulting from thermal effects are generally self-relieving, that is thermal forces and moments are greatly reduced or completely relieved once concrete cracks or reinforcement yields; as a result, thermal effects do not reduce the strength of a section for mechanical loads. For example, assuming a fixed-end beam under transverse loads would produce negative moments at the ends and a positive moment at the center. It is also assumed that the transverse load is such that the negative moment reinforcement is near yield (for example, at 99% of yield). If the temperature is increased at the bottom of the beam, introducing a thermal gradient over its entire length, this gradient would cause additional negative moment. When the negative moments increase by 1%, the reinforcement would start yielding. The negative moments at the ends, however, cannot increase beyond 100% because the reinforcement is already yielded. Thus, it can be said that the thermal moments at the ends are relieved as soon as the reinforcement yields. Yet, the structure remains stable because the lateral load does not change. Therefore, simplifying assumptions and approximations in analyses are acceptable. Although it is not feasible to set definitive rules regarding these assumptions and approximations, some general guidelines are presented. These guidelines are based on experience with thermal analyses and engineering judgment.

- Design for thermal effects is primarily for serviceability and should address control of cracking;
- Extreme environmental events (that is, E_{ss} and W_t) are rare occurrences. Serviceability of the structure may not be required after such events. If they occur, high stresses are induced in local areas. Under these stresses, concrete cracks and reinforcement may yield, relieving thermally induced stresses. Thus, it may be too conservative to add the thermal stresses based on elastic analysis to the stresses due to extreme environmental loads. Consequently, the elastically calculated thermal stresses should be reduced considering concrete cracking and reinforcement yield before combining them with the stresses from extreme environmental loads;
- In nuclear power structures, the controlling load combinations are generally those that include E_o or E_{ss}. These load cases provide sufficient reinforcement to control cracking. It would be counterproductive to add reinforcement to mitigate thermal effects because the additional reinforcement would stiffen the structure, thus increasing the stresses due to thermal effects. This is unnecessary because thermal effects typically self-relieve without the need for additional reinforcement. If additional thermal reinforcement is indicated by the design and analysis, the appropriateness of methods and means should be re-evaluated;
- Thermal gradients should be considered in the design of reinforcement for normal conditions to control cracking. Thermal gradients less than approximately 100 °F (56 °C) need not be analyzed because such gradients will not cause significant stress in the reinforcement or strength deterioration. It may cause a small incursion into the nonlinear range for extreme events, but such incursions are not likely to adversely affect the overall behavior of the structure. Because thermal gradient results in flexural stress, the minimum reinforcement on the tension face should be established assuming this face is in flexural tension.

  The change in curvature due to thermal gradient is approximated by $\phi_A = \alpha\Delta T/t$. The maximum additional strain in reinforcement due to the change in curvature can be approximated by $\varepsilon_c = \phi_A t = \alpha\Delta T$. This approximation is

for a beam element; for a plate element, the change of curvature will be somewhat higher due to Poisson's ratio, that is, $\phi_A = \alpha\Delta T/[t(1 - \nu)]$. This approximation conservatively assumes rotation of the section about the outside compression face. With $\alpha \approx 6 \times 10^{-6}$ in./in./°F (1.1×10^{-5} mm/mm/°C) and $\Delta T = 100$ °F (56 °C), the additional reinforcement strain will be about 600 μin./in. (600 μmm/mm), or 0.0006 in./in. (0.0006 mm/mm), which corresponds to about $0.3\varepsilon_y$ for 60 ksi (420 MPa) steel (because $\varepsilon_y = \sigma_y/E_s$ = (60 ksi)/(29,000 ksi) = 0.002. Therefore, the thermal strain, relative to yield strain, due to a thermal gradient of $\Delta T = 100$ °F (56 °C), is [(0.0006)/(0.002)] = 0.3 or $0.3\varepsilon_y$). If the reinforcement strain is equal to $0.9\varepsilon_y$ without the thermal effect, the total strain with the thermal gradient will be approximately $1.2\varepsilon_y$, or about 20% beyond yield. Such an exceedance is inconsequential (Gurfinkel 1972), and will not reduce the capacity of the concrete section for mechanical loads.

- Similarly, the maximum additional concrete strain can be estimated for a fully constrained component to be also approximately 0.0006 in./in. (0.0006 mm/mm), which is only about 20% of the maximum design concrete strain of 0.003. Again, such a small exceedance in the extreme fiber of the cross section will not be detrimental to the overall strength of the structure; and
- A uniform temperature change ($T_m - T_b$) of 50 °F (28 °C) or less need not be analyzed. Such a temperature change may cause up to about 0.0003 in./in. (0.0003 mm/mm) strain, which is only 10% of the maximum design concrete strain of 0.003. (Note: The referenced text is intended for concrete in compression. The 10% strain refers to the concrete ultimate strain, which is generally accepted as 0.003. In real structures, the maximum concrete strain will be significantly less than 0.002, which is the strain at the peak concrete stress in the Hognestad stress-strain curve [Kohli and Gurbuz 1976]. Thus, a practical strain limit in the example problem will increase from 0.002 to 0.0023, which is still less than the ultimate concrete strain.) Minimum reinforcement should be established using the requirements for flexural tension.

In the determination of forces and moments resulting from thermal effects, it would be theoretically possible to perform analyses with precise stiffness and stress-strain information on all structural materials. Fortunately, however, such a burdensome effort is not necessary. The aforementioned guidelines are general; there may be cases where the effect of the thermal effects may be more significant on a critical part of the structure due to layout of the structure. The engineer should review the temperature distribution in the structure and address the potential effects on a case-by-case basis.

1.4—Analysis techniques

There are several well-recognized techniques for the analysis of thermal effects in structures, from both steady-state and transient (time-dependent) temperature profiles. Determination of a steady-state or transient design-and-analysis approach is based on the initial condition of the structure in question and process conditions related to plant operations and the natural environment (for example, temperature source and exposure time data).

1.4.1 *Hand calculations*—Many thermal exposure conditions can be solved by hand calculations, especially where the initial conditions are relatively uncomplicated or the structure considered is simple in configuration and behavior. It is possible to look at both steady-state and time-dependent solutions in this manner. Simplified hand-calculation approaches are still valuable today (the examples presented in Chapters 3 and 4 are based on such calculations), particularly in the confirmation of computer-based analysis results.

1.4.2 *Computer-based analysis*—Use and capability of computers and software in structural design has expanded greatly since the time when the early nuclear power plants were designed. Computer analysis methods can be broadly classified by the modeling and algorithm used, with the two most prevalent systems involving: 1) stiffness matrix or finite element method consisting of linear elements (for example, linear beam elements); and 2) finite element method consisting of two- (for example, plate elements) or three-dimensional elements (for example, brick elements). Both linear elements and finite elements can be used to accurately model a concrete structure and its components, to input applied mechanical loads and effects such as thermal gradients, and to produce an output of resultant forces, moments, stresses, and deformations representative of the modeled structure based on mechanics and code requirements. Programs written around linear elements are particularly useful for frame-type structures to determine the transfer of loads to connected components. Many existing computer programs contain embedded design code (for example, ACI 318) requirements to support proportioning and reinforcement definition. Such programs allow the introduction of thermal gradients, with resulting forces and moment computation due to restraints, and certain programs have the ability to examine nonlinear response. Analyzing the impacts of cracking on structural capacity and stiffness, however, is generally beyond the capabilities of this software program type.

Finite element analysis (FEA) involves a more detailed simulation of a structure, which is geometrically divided into a mesh of two- or three-dimensional elements for a greater precision in assessment of force and displacement distribution within the structure. The input model also includes boundary conditions and mechanical loading data. Finite element models can be used for structural analysis and design, as well as for assessing steady-state and transient temperature effects and heat transfer. FEA methods can be used for both static and dynamic analysis and refined assessment of nonlinear response. FEA methods are capable of analyzing both steady-state and transient thermal effects in reinforced concrete.

Elastic FEAs can be used with a reduced elastic modulus for concrete to account in a very simple manner for the various effects of cracking, creep, and yield. Values of $0.50E_c$ have been used in past practice.

Nonlinear thermal analysis is useful where the material properties in a structure change with exposure to elevated temperatures, such as those listed in Appendix E.4.2 and

E.4.3 of ACI 349-06. For instance, the specific heat capacity of steel rises with elevated temperature exposure, whereas mechanical properties decrease. Concrete compressive strength typically decreases, particularly where the exposure is either long-term or locally severe. Other nonlinear schemes will involve the change in radiative and convective properties as temperatures vary.

1.5—Consideration of thermal effects in analysis

Structural analysis for most nuclear plant concrete structures involves the determination of whether or not thermally induced forces or moments may occur as a result of restraint. A typical prerequisite step in completing the structural analysis and design of a structure is the determination of temperature boundary conditions, temperature ranges (bulk temperature change), and gradients. Considerations include:

- Thermal conduction. The assessment of temperatures at given locations in concrete structures. The temperature distribution could be calculated either as a steady state or a transient, depending on the exposure;
- Temperature-induced stress. The temperature distribution can be used to determine the elastic thermal stresses throughout the structure; and
- Fire protection. Thermal analysis can be used to establish the temperature/time relationship influencing a structure subjected to fire. The analysis can take account of fire barriers and protective materials such as intumescent coatings and fireboards.

Thermal effects in combination with mechanical loads often lead to structural cracking of concrete that could adversely affect corrosion protection of the reinforcement. The thermal assessment should consider the possibility that, under certain extreme conditions, thermal movements could significantly affect the behavior of the structure. In components or systems that include variable temperature exposure, mechanical loads, and restraint against displacement, the support requirements for each of the loading schemes may be mutually exclusive. A structure designed to restrict displacement-induced stresses due to vibration or bracing may provide greater end fixity than desired, resulting in elevated thermally induced stresses. A combined thermal and structural analysis using FEA programs is typically needed to balance the requirements.

1.6—Stiffness and deformation effects

As structural components such as concrete slabs and walls are exposed to significant levels of stressing and cracking as a result of restrained thermal deformations, reductions in stiffness due to said cracking and thermal creep can cause rapid decay in the restraint forces developed, and deformation can increase. Simplified approaches, such as use of cracked section properties and moment of inertia, can be used to calculate the resultant deflections using empirical formulas per ACI 207.2R, 209R, and 435.7R, and Fu and Daye (1991).

Nonlinear finite element analysis procedures may also be employed to investigate the theoretical response and deformations in such components. Simulations of the component response can be obtained. Important to achieving accurate results are the consideration of tension-stiffening effects, strain-softening effects (treatment of negative strain), and out-of-plane shear. Selection of software for use in thermal analysis should consider compatibility with modeling concrete (certain programs are suited for homogeneous materials only), ability to handle strain-softening, user capability and software experience base, and status of verification with respect to 10CFR50 Appendix B requirements (Office of the Federal Register 2002).

1.7—Summary

Thermal effects can cause forces and moments in a reinforced concrete structure due to restraint of thermal expansion and contraction. Because concrete resistance to tension is low, the concrete cracks under the thermally induced tensile stresses. As concrete cracks, these tensile stresses are relieved. Although rarely a design concern from a strength perspective, the serviceability of a structure exposed to thermal effects may ultimately be of concern, and such cases should be correctly identified in the assessment and considered in the design.

Accurate analysis of thermal effects, mechanical loads, restraint, concrete cracking, and other stress-relieving effects are difficult at best. The use of a simplified procedure should be adequate to calculate the thermal effects. If further examination is warranted, computer programs are available to deal with the issue more effectively. Specific design methods associated with frame and axisymmetric structures are contained in this report.

CHAPTER 2—NOTATION AND DEFINITIONS

2.1—Notation

A_s = area of tension reinforcement within width b, in.^{2} (mm^2)

A'_s = area of compression reinforcement within width b, in.^{2} (mm^2)

a = length of cracked end of component at which stiffness coefficient and carryover factor are determined, for example, in a end-cracked beam (Fig. 3.3 through 3.6) or interior-cracked beam (Fig. 3.7 through 3.10), a is length of uncracked end of component at which stiffness coefficient and carryover factor are determined, in. (mm)

b = width of rectangular cross section, in. (mm)

CO = cracked component carryover factor from end of the component to opposite end

CO_{AB} = cracked component carryover factor from End A to End B

CO_{BA} = cracked component carryover factor from End B to End A

DF = distribution factor

d = distance from extreme fiber of compression face to centroid of tension reinforcement, in. (mm)

d' = distance from extreme fiber of compression face to centroid of compression reinforcement, in. (mm)

E_c = modulus of elasticity of concrete, psi (MPa)

E_o = load effects of operating basis earthquake (OBE) or related internal moments and forces, including OBE-induced piping and equipment reactions

E_s = modulus of elasticity of reinforcing steel, psi (MPa)
E_{ss} = load effects of safe shutdown earthquake (SSE) or related internal moments and forces, including SSE-induced piping and equipment reactions
e = eccentricity of internal force N on the rectangular section, measured from section centerline, in. (mm)
F = flexural coefficient, in.-lb: $bd^2/12{,}000$ (SI: $bd^2/1000$) (ACI Committee 340 1997)
f_c = final cracked section extreme fiber compressive stress resulting from internal section forces M, N, and ΔT, psi (MPa)
f'_c = specified compressive strength of concrete, psi (MPa)
f_{cL} = cracked section extreme fiber compressive stress resulting from internal forces M and N, psi (MPa)
f_r = modulus of rupture of concrete, psi (MPa)
f_y = specified yield strength of reinforcing steel, psi (MPa)
I_{cr} = cracked section moment of inertia about centroid of cracked rectangular section, in.^{4} (mm^4)
I_g = uncracked section moment of inertia (excluding reinforcement) about centerline of rectangular section, in.^{4} (mm^4)
j = ratio of distance between centroid of compression and centroid of tension reinforcement to depth d
K = cracked component stiffness at End a (pinned), with opposite end fixed
K_A = cracked component stiffness at End A (pinned), with opposite end fixed
K_B = cracked component stiffness at End B (pinned), with opposite end fixed
K_u = strength coefficient for resistance = $f'_c\,\omega(1 - 0.59\omega)$, where $\omega = \rho f_y/f'_c$, psi (MPa) (ACI Committee 340 1997)
k = ratio of depth of triangular compressive stress block to depth d, resulting from internal section forces M, N, and ΔT
kd = neutral axis location on section due to N, M, and ΔT (Fig. 4.1), in. (mm)
k_L = ratio of depth of triangular compressive stress block to depth d, resulting from internal section forces M and N
k_Ld = neutral axis location on section due to N and M (Fig. 4.1), in. (mm)
k_s = dimensionless stiffness coefficient = KL/E_cI_g
L = total length of component, in. (mm)
L_T = cracked length of component, in. (mm)
M = internal moment at section centerline due to factored mechanical loads, including factored moment due to $T_m - T_b$, in.-lb (mm·N)
$\overline{M}$ = final internal moment at section centerline resulting from M and ΔT, in.-lb (mm·N)
M_{cr} = cracking moment = $bt^2f_r/6$, in.-lb (mm·N)
M_{FE} = cracked component fixed-end moment due to ΔT or $T_m - T_b$, at end a, in.-lb (mm·N)
M_u = moment capacity of section, ft-kips (mm·N)
$M_{\Delta T}$ = thermal moment due to ΔT, $M_{\Delta T} = \overline{M} - M$, in.-lb (mm·N)
N = internal axial force at section centerline due to factored mechanical loads, including factored axial force due to $T_m - T_b$, kips (N)
n = modular ratio = E_s/E_c
T_b = base (stress-free) temperature, °F (°C)
T_m = mean temperature, °F (°C)
t = thickness of rectangular section, in. (mm)
W_t = loads generated by design basis tornado (DBT), or related internal moments and forces
α = concrete coefficient of thermal expansion, in./in./°F (mm/mm/°C)
Δ = transverse displacement difference between ends of cracked component due to $T_m - T_b$ acting on adjoining components, in. (mm)
ΔT = linear temperature gradient, ºF (ºC)
ε_c = final cracked section strain at extreme fiber of compression face = $\varepsilon_{cL} + \varepsilon_{cT}$
ε_{cL} = cracked section strain at extreme fiber of compression face resulting from M, N, and ΔT
ε_{cT} = concrete strain in compression face due to ΔT (Fig. 4.1)
ϕ = final cracked section curvature change = $\phi_L + \phi_T$
ϕ_A = curvature due to thermal gradient
ϕ_L = cracked section curvature change resulting from internal forces M and N
ϕ_T = cracked section curvature change required to return free thermal curvature $\alpha\Delta T/t$ to 0
ν = Poisson's ratio of concrete
ρ = ratio of tension reinforcement = A_s/bd
ϕ' = ratio of compression reinforcement = A'_s/bd

2.2—Definitions

base temperature—the temperature at which a concrete member is cured. This is the temperature at which it is assumed the material is free of thermal stresses.

mechanical load—loads that cause stresses in elements to maintain equilibrium, such as gravity, earthquake and wind loads, and pressures. Loads due to geometric constraints (including thermal, settlement, creep, and shrinkage effects) are not considered mechanical loads as the resulting stresses are relieved when the constraint is removed. For example, an axial load applied to a column will cause stresses. On the other hand, uniform temperature increase will not cause stresses unless the column is restrained from axial deformation. Another example: internal pressure in a cylinder will cause stresses in the walls and ends. If the cylinder is subjected to uniform temperature increase, no stresses will be induced unless the expansion is restrained.

safety-related concrete structures—safety-related concrete structures are structures that are designed to remain functional under the design loads. These structures support, house, or protect nuclear safety class systems or components.

secondary stress—a self-limiting normal or shear stress that is caused by the constraint of a structure and that is expected to cause minor distortions that would not result in a failure of the structure.

self-relieving—the process by which excessive internal pressure (stress) is automatically relieved.

temperature distribution—the variation of the total temperature across a section at a point in time. The temperature distribution across a section can vary with time as well as varying along the length of the member. For such variations, the engineer should evaluate the effects of temperature distribution at a number of sections and for a number of time durations.

CHAPTER 3—FRAME STRUCTURES

3.1—Scope

The thermal effect on the frame is assumed to be represented by temperatures that vary linearly through the thicknesses of the components. The linear temperature distribution for a specific component must be constant along its length. Each such distribution can be separated into a gradient ΔT and into a temperature change with respect to a base (stress-free) temperature $T_m - T_b$.

Frame structures are characterized by their ability to undergo significant flexural deformation under these thermal effects. They are distinguished from the axisymmetric structures discussed in Chapter 4 by the ability of their structural components to undergo rotation, such that the free thermal curvature change of $\alpha\Delta T/t$ is not completely restrained. The thermal moments in the components are proportional to the degree of restraint. In addition to frames, slabs and walls may fall into this category.

The aforementioned rotational feature is automatically considered in a structural analysis using uncracked component properties. An additional reduction of the component thermal moments, however, can occur if component cracking is taken into account. Sections 3.2 and 3.3 of this chapter describe criteria for the cracking reduction of component thermal moments. These criteria can be used as the basis for an analysis of the structure under thermal effects, regardless of the method of analysis selected. In Section 3.4, these criteria are applied to the moment distribution analysis method.

There are frame and slab structures that can be adequately idealized as frames of sufficient geometric simplicity to lend themselves to moment distribution. Even if an entire frame or slab structure does not permit a simple idealization, substructures can be isolated to study thermal effects. Often, with the use of computer programs for the analysis of complex structures, a feel for the reasonableness of the results is attainable only through less complex analyses applied to substructures. The moment distribution method for thermal effects is applicable for this work. This design approach uses cracked component stiffness coefficients and carryover factors. These depend on the extent of component cracking along its length due to mechanical loads, as discussed in Section 3.3.

3.2—Section cracking

Simplifying assumptions are made as follows for the purpose of obtaining the cracked section thermal moments and the section (cracked and uncracked) stiffnesses. The fixed-end moments, stiffness coefficients, and carryover factors of Section 3.4 are based on these assumptions:

1. Concrete compression stress is taken to be linearly proportional to strain over the component cross section;

2. For an uncracked section, the moment of inertia is I_g, where I_g is based on the gross concrete dimensions and the reinforcement is excluded. For a cracked section, the moment of inertia is I_{cr}, where I_{cr} is referenced to the centroidal axis of the cracked section. In the formulation of I_{cr}, the compression reinforcement is excluded and the tension reinforcement is taken to be located at the tension face; that is $d = t$ is used; and

3. The axial force on the section due to mechanical loads and thermal effects is assumed to be small relative to the moment ($e/d \geq 0.5$). Consequently, the extent of section cracking is taken as that which occurs for a pure moment acting on the section.

The first assumption is strictly valid only if the extreme fiber concrete compressive stress due to combined mechanical loads and thermal effects does not exceed $0.5f'_c$. At this stress, the corresponding concrete strain is around 0.0005 in./in. (0.0005 mm/mm). For extreme fiber concrete compressive strains greater than 0.0005 in./in. (0.0005 mm/mm) but less than 0.001 in./in. (0.001 mm/mm), the differences are insignificant between a cracked section thermal moment based on the linear assumption adopted herein versus a nonlinear concrete stress-strain relationship such as that described in Fu and Daye (1991), Gurfinkel (1972), and Kohli and Gurbuz (1976). Consequently, cracked component thermal moments given by Eq. (3-3) and (3-4) are sufficiently accurate for concrete strains not exceeding 0.001 in./in. (0.001 mm/mm).

For concrete strains greater than 0.001 in./in. (0.001 mm/mm), the equations previously identified will result in cracked component thermal moments that are greater than those based on the nonlinear theory. In this regard, the thermal moments are conservative. They are, however, still reduced from their uncracked values. This cracking reduction of thermal moments can be substantial, as discussed in Section 4.1, which also incorporates Assumption 1.

Formulation of the thermal moments based on a linear concrete stress-strain relationship allows the thermal moments to be expressed simply by the equations in Chapter 3, or by the normalized thermal moment graphs of Chapter 4. Such simplicity is desirable in a designer-oriented approach.

Regarding I_{cr} in Assumption 2, the assumptions for the compression and tension reinforcement result in the simple expression of $(6jk^2)I_g$ for I_{cr} if the axial load is small, as specified in Assumption 3. The use of $(6jk^2)I_g$ will overestimate the cracked section moment of inertia of sections, for which $e/d \geq 0.5$, either with or without compression reinforcement. For a component with only tension reinforcement typically located at $d = 0.9t$, the actual cracked section moment of inertia is overestimated by 35% ($I_g = (1/12)bt^3$; $I_{g1} = (1/12)b(0.9t)^3$; $I_g/I_{g1} \approx 1.35$), regardless of the amount of reinforcement. For a component with equal amounts of compression and tension reinforcement, located at $d' = 0.1d$ and $d = 0.9t$, its actual cracked section moment of inertia is also overestimated. The overestimation will vary from 35% at the lower reinforce-

ment ratio ($\rho' n = \rho n = 0.02$) down to 15% at the higher values ($\rho' n = \rho n = 0.12$).

The use of $(6jk^2)I_g$ for cracked sections and the use of I_g for uncracked sections are further discussed relative to component cracking in Section 3.3.

Regarding Assumption 3, the magnitude of the thermal moment depends on the extent of section cracking as reflected by I_{cr}. I_{cr} depends on the axial force N and moment M. The relationship of I_{cr}/I_g versus e/d, where $e = M/N$, is shown in Fig. 3.1. The eccentricity e is referred to the section centerline. In Fig. 3.1, it is seen that for $e/d \geq 1$, I_{cr} is practically the same as that corresponding to pure bending. For $e/d \geq 0.5$, the associated I_{cr} is within 10% of its pure bending value. Most nonprestressed frame problems are in the $e/d \geq 0.5$ category. Consequently, for these problems, it is accurate within 10% to use the pure bending value of $(6jk^2)I_g$ for I_{cr}. This is the basis of Assumption 3.

3.3—Component cracking

Ideally, a sophisticated analysis of a frame or slab structure subjected to both mechanical and thermal effects might consider concrete cracking and the resulting changes in component properties at many stages of the load application. Such an analysis would consider the sequential application of the loads and effects, and cracking would be based on the modulus of rupture of the concrete f_r. The loads would be applied incrementally to the structure. After each load increment, the section properties would be revised for those portions of the components that exhibit extreme fiber tensile stresses in excess of f_r. The properties of the components for a given load increment would reflect the component cracking that had occurred under the sum of all preceding load increments and effects. In such an analysis, the internal forces and moments would result in component cracking, with only the results from thermal effects considered relieved.

The type of analysis summarized previously is consistent with the approach in Item 2 of Section RE.3.3 of the Commentary to Appendix E of ACI 349-06. An approximate analysis, but one that is generally conservative for the thermal effects, is also suggested in the Commentary to Appendix E of ACI 349 (Item 3 of Section RE.3.3) as an alternative. This alternate analysis considers the structure to be uncracked under the mechanical loads and to be cracked under the thermal effects. The results of an analysis of the uncracked structure under mechanical loads are combined with the results of an analysis of the cracked structure under the thermal effects. A simplified method of analysis is discussed that will yield cracked component thermal moments that are conservative for most practical problems.

The extent of cracking that the components experience under the total mechanical load (including the specified load factors) forms the basis for the cracked structure used for the thermal effects analysis. Cracking will occur wherever the mechanical load moments exceed the cracking moment M_{cr}. The addition of thermal moments that are the same sign as mechanical moments will increase the extent of cracking along the component length. Recognizing this, in many cases, it is conservative for design to consider the component to be cracked wherever tensile stresses are produced by the mechanical loads if these stresses would be increased by the thermal effects. The addition of thermal moments that are of opposite sign to the mechanical moments that exceed M_{cr}, however, may result in a final section that is uncracked. Therefore, for simplicity, the component is considered to be uncracked for the thermal effect analysis wherever along its length the mechanical moments and thermal moments are of opposite sign.

Two types of cracked components will result: 1) end-cracked; and 2) interior-cracked. The first type occurs for cases where mechanical and thermal moments are of like sign at the component ends. The second type occurs where these moments are of like sign at the interior of the component. Stiffness coefficients, carryover factors, and fixed-end thermal moments are developed for these two types of components in Section 3.4. A comprehensive design example is presented in Section 3.5.

The aforementioned simplification of considering the component to be uncracked wherever the mechanical and thermal moments are of opposite sign is conservative due to the fact that the initial portion of a thermal effect, such as ΔT, will actually act on a section that may be cracked under the mechanical loads. Consequently, the fixed-end moment due to this part of ΔT will be that due to a component completely cracked along its length. Once the cracks close, the balance of ΔT will act on an uncracked section. Consideration of this two-phase aspect makes the problem more complex. The conservative approach adopted herein removes this complexity. Some of the conservatism, however, is reduced by the use of I_g for the uncracked section (Assumption 2) rather than its actual uncracked section stiffness, which would include reinforcement, and is substantially greater than I_g for $\rho n \geq 0.06$.

The fixed-end moments depend not only on the cracked length L_T, but also on the location of the cracked length a along the component. This can be seen from a comparison of the results for an end-cracked component and an interior-cracked component for the same value of L_T. The method discussed in Section 3.4 accounts for this. This approach is more applicable for the determination of the thermal moments than the use of an effective moment of inertia for the entire component length. The concept of a single effective moment of inertia for purposes of component deflection calculation has resulted in Eq. (9-10) of ACI 349-06. This equation is empirically based and, as such, accounts for: 1) partially cracked sections along the component; and 2) the existence of uncracked sections occurring between flexural cracks. These two characteristics are indirectly provided for (to an unknown extent) by the use of $(6jk^2)I_g$, which overestimates the cracked section moment of inertia by the amount described previously.

3.4—Cracked component fixed-end moments, stiffness coefficients, and carryover factors

The thermal moments due to the linear temperature gradient ΔT and those resulting from the expansion or contraction of the axis of the component $T_m - T_b$ are considered separately. For each type of thermal effect, fixed-end

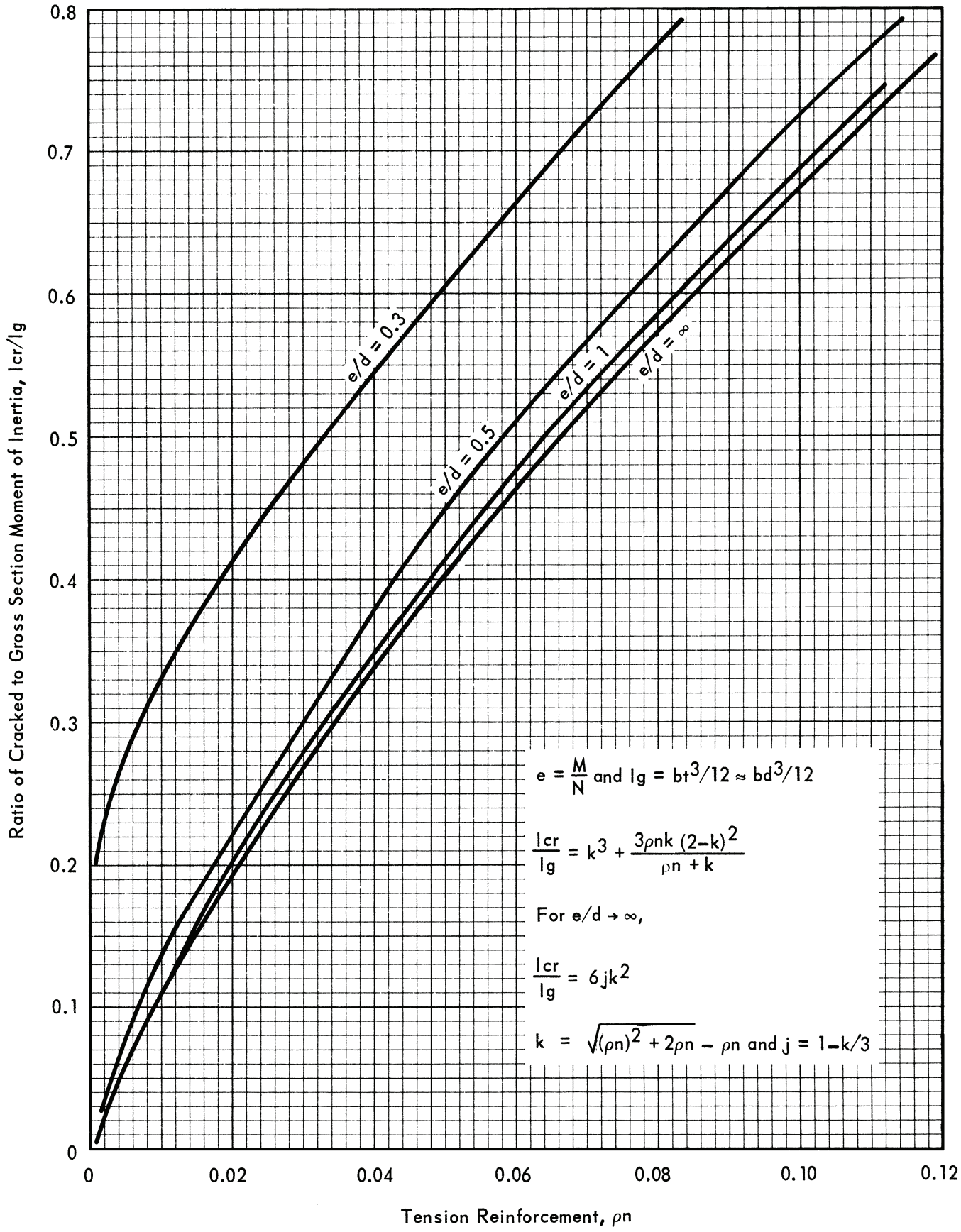

Fig. 3.1—Effect of axial force on cracked section moment of inertia (no compression reinforcement).

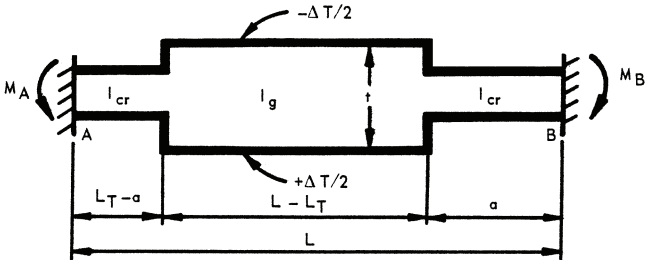

Fig. 3.2(a)—ΔT fixed-end moments: member cracked at ends by mechanical loads.

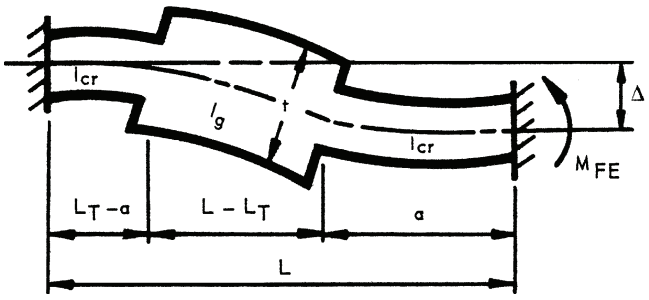

Fig. 3.2(b)—$T_m - T_b$ fixed-end moment: member cracked at ends by mechanical loads.

moments, stiffness coefficients, and carryover factors were obtained for two types of cracked components: 1) end-cracked; and 2) interior-cracked. The first type applies to cases where mechanical and thermal effects produce moments of like sign at component ends. The second type applies to cases where mechanical and thermal effects produce moments of like sign in the interior of the component.

These factors are presented for the case of an end-cracked component in Fig. 3.2(a)

$$M_A = \left(\frac{\alpha \Delta T L}{2t}\right) K_A (1 - CO_{AB})$$
$$M_B = \left(\frac{\alpha \Delta T L}{2t}\right) K_B (1 - CO_{BA}) \quad (3\text{-}1)$$

Although shown only for a component cracked at the ends, the aforementioned expressions for M_A and M_B also apply to a component cracked in its interior.

In Eq. (3-1), $\alpha\Delta TL/2t$ = the angle change of the component ends with the rotational restraints removed; K_A = the stiffness of the component at A with B fixed ($4E_cI_g/L$ for uncracked component); K_B = the stiffness of the component at B with A fixed ($4E_cI_g/L$ for the uncracked component); CO_{AB} = the carryover factor from A to B (1/2 for uncracked component); and CO_{BA} = the carryover factor from B to A (1/2 for uncracked component).

The expressions for K and CO can be derived from moment-area principles. Also, K can be expressed as

$$K = \frac{E_c I_g}{L} k_s \quad (3\text{-}2)$$

where k_s is the dimensionless stiffness coefficient that is a function of L_T/L and a/L_T. Likewise, CO can be expressed as a function of L_T/L and a/L_T.

Figures 3.3 through 3.6 show k and CO for selected values of L_T/L and a/L_T that should cover most practical problems. In these figures, k_s is given at the end, which is cracked a distance a, and CO is the carryover factor from this end to the opposite end. Intermediate values of k_s and CO can be determined by linear interpolation of these curves.

For a component cracked a distance L_T in its interior, k_s and CO are determined from Fig. 3.7 through 3.10. k_s is the stiffness coefficient at the end that is uncracked a distance a. CO is the carryover factor from this end to the opposite end.

Based on the previous discussion, the ΔT fixed-end moment at the a end of the component can be expressed as

$$M_{FE} = \frac{E_c \alpha \Delta T b t^2 k_s (1 - CO)}{12} \frac{}{2} \quad (3\text{-}3)$$

For the purpose of determining the mean temperature effects, it is necessary to develop the $T_m - T_b$ fixed-end moment, which is shown in Fig. 3.2(b) for a component cracked at its ends.

The $T_m - T_b$ fixed-end moment at the end cracked a distance a is

$$M_{FE} = \frac{E_c I_g \Delta}{L^2} k_s (1 + CO) \quad (3\text{-}4)$$

where k_s and CO are same as that defined previously. The displacement Δ is produced by $T_m - T_b$ acting on an adjacent component. The comprehensive design example of Section 3.5 illustrates this.

3.5—Frame design example

The continuous frame shown in Fig. 3.11 is given with all components 1 ft wide x 2 ft thick and 3 in. cover on the reinforcement. The load combination to be considered is $U = D + L + T_o + E_{ss}$.

The mechanical loading consists of

$$W_D = 406 \text{ lb/ft}$$

$$W_L = 680 \text{ lb/ft}$$

on component BC, and a lateral load of 3750 lb at joint C due to E_{ss}.

The thermal gradient T_o results from 130 °F interior and 50 °F exterior temperature. Thus, $T_m = (130 + 50)/2 = 90$ °F. The base temperature T_b is taken as 70 °F. For this condition, $T_m - T_b = 90$ °F – 70 °F = +20 °F and $\Delta T = 80$ °F (hot interior, cold exterior).

The material properties are $f'_c = 3000$ psi and $E_c = 3.12 \times 10^6$ psi, $f_y = 60{,}000$ psi and $E_s = 29 \times 10^6$ psi; and $\alpha = 5 \times 10^{-6}$ in./in./°F. Also, $n = E_s/E_c = 9.3$.

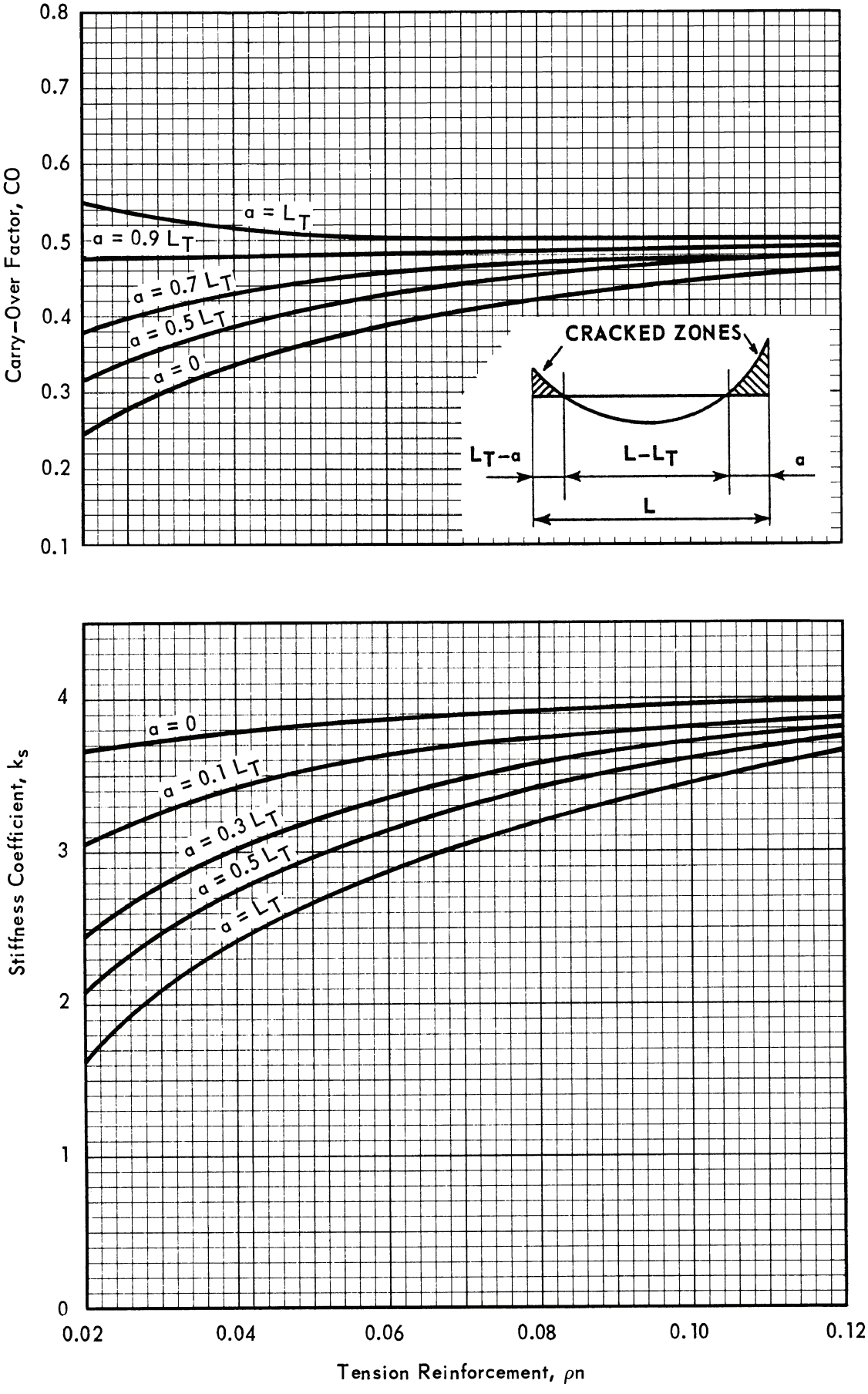

Fig. 3.3—End-cracked beam, k_s *and* CO *for* $L_T = 0.1L$.

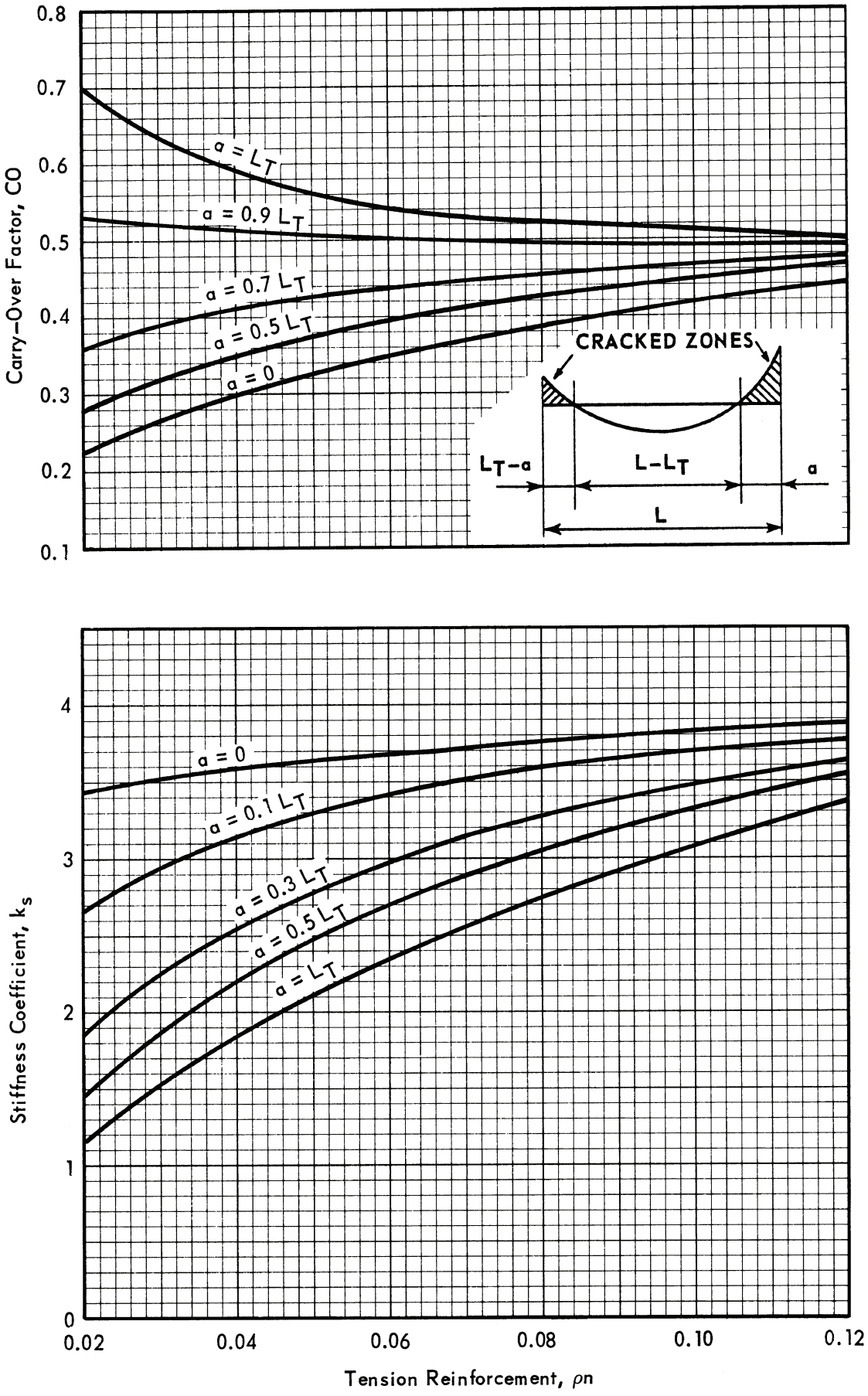

Fig. 3.4—End-cracked beam, k_s *and* CO *for* $L_T = 0.2L$.

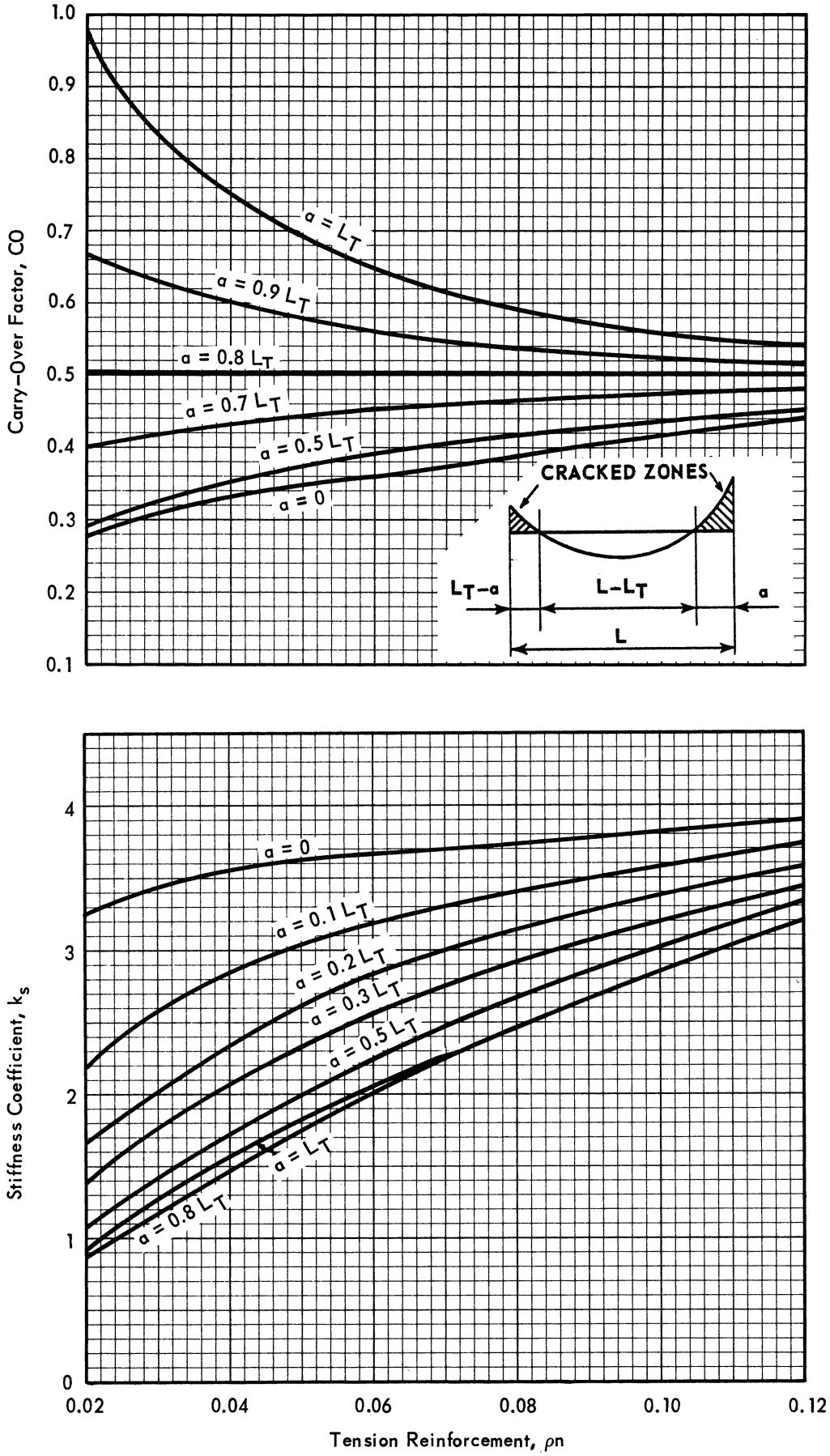

Fig. 3.5—End-cracked beam, k_s *and* CO *for* $L_T = 0.4L$.

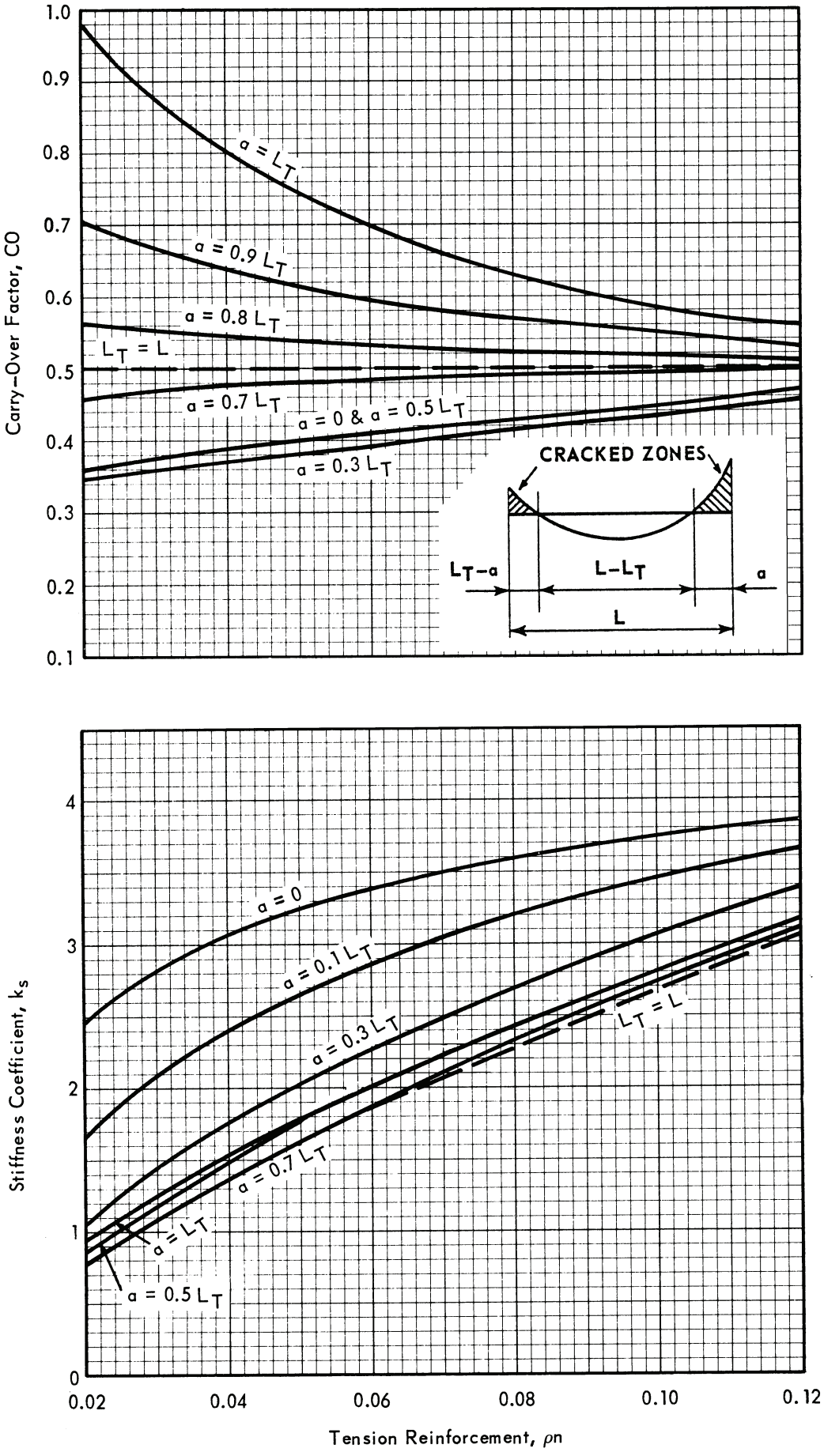

Fig. 3.6—End-cracked beam, k_s *and* CO *for* $L_T = 0.6L$.

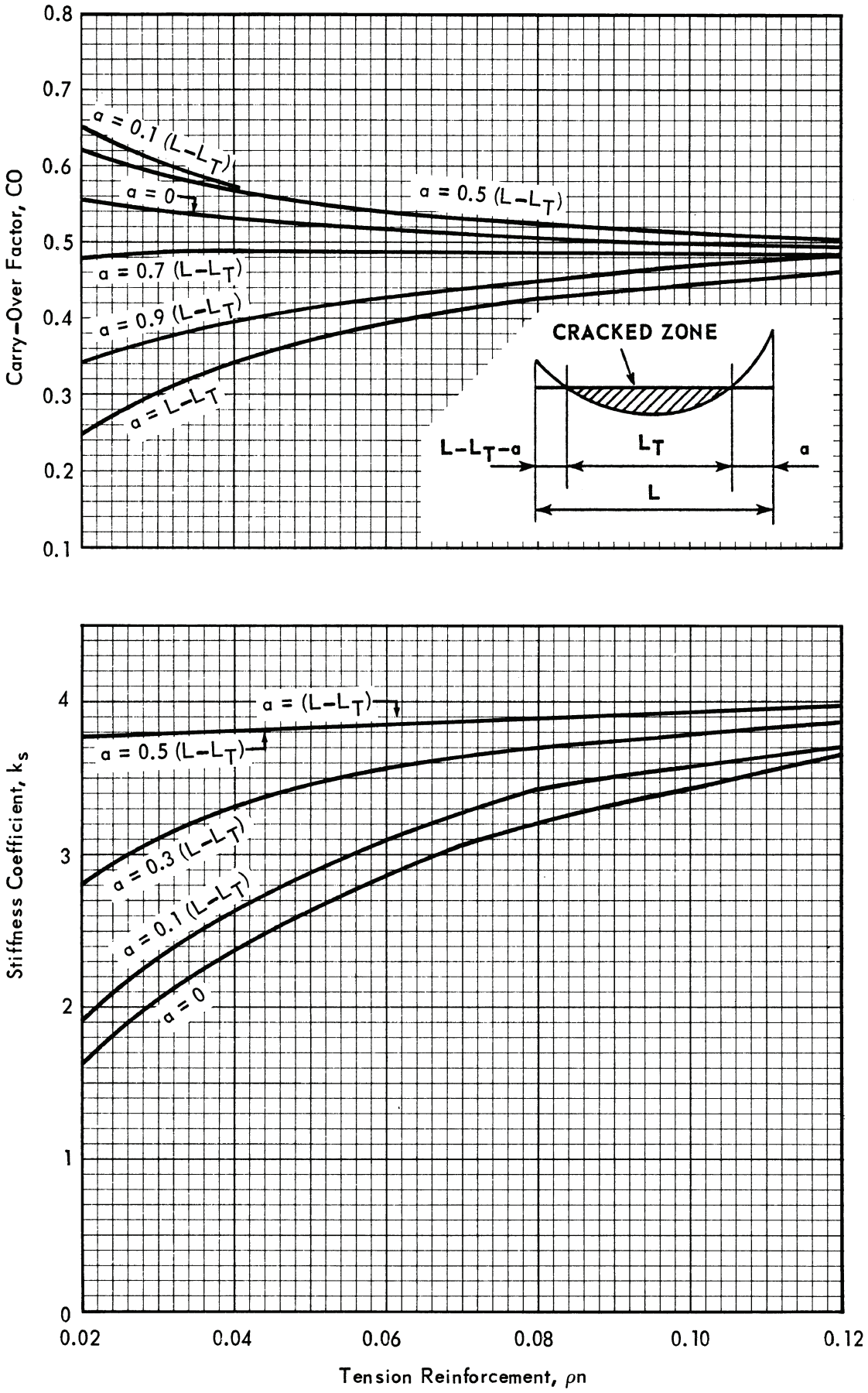

Fig. 3.7—Interior-cracked beam, k_s *and* CO *for* $L_T = 0.1L$.

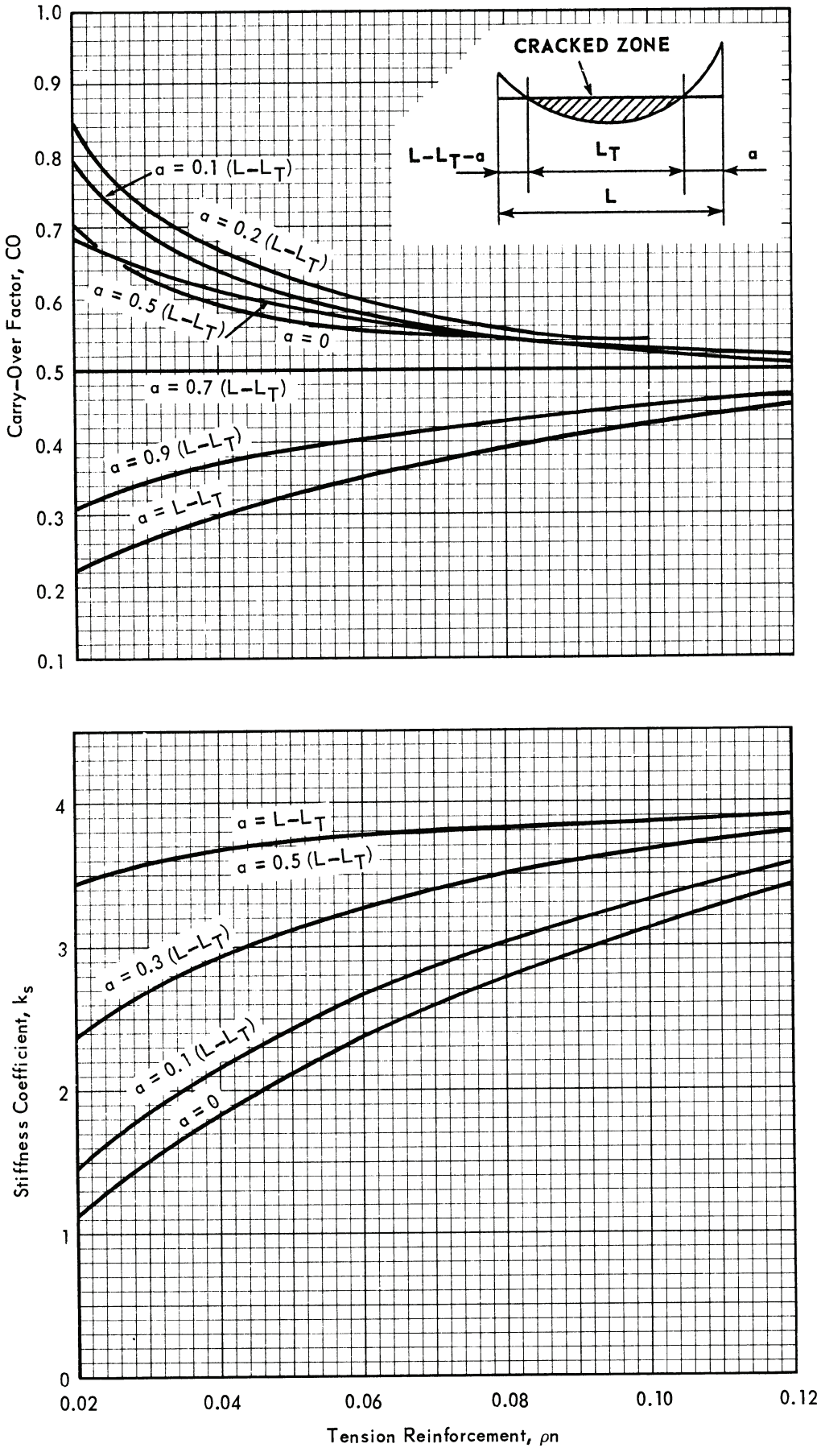

Fig. 3.8—Interior-cracked beam, k_s *and* CO *for* $L_T = 0.2L$.

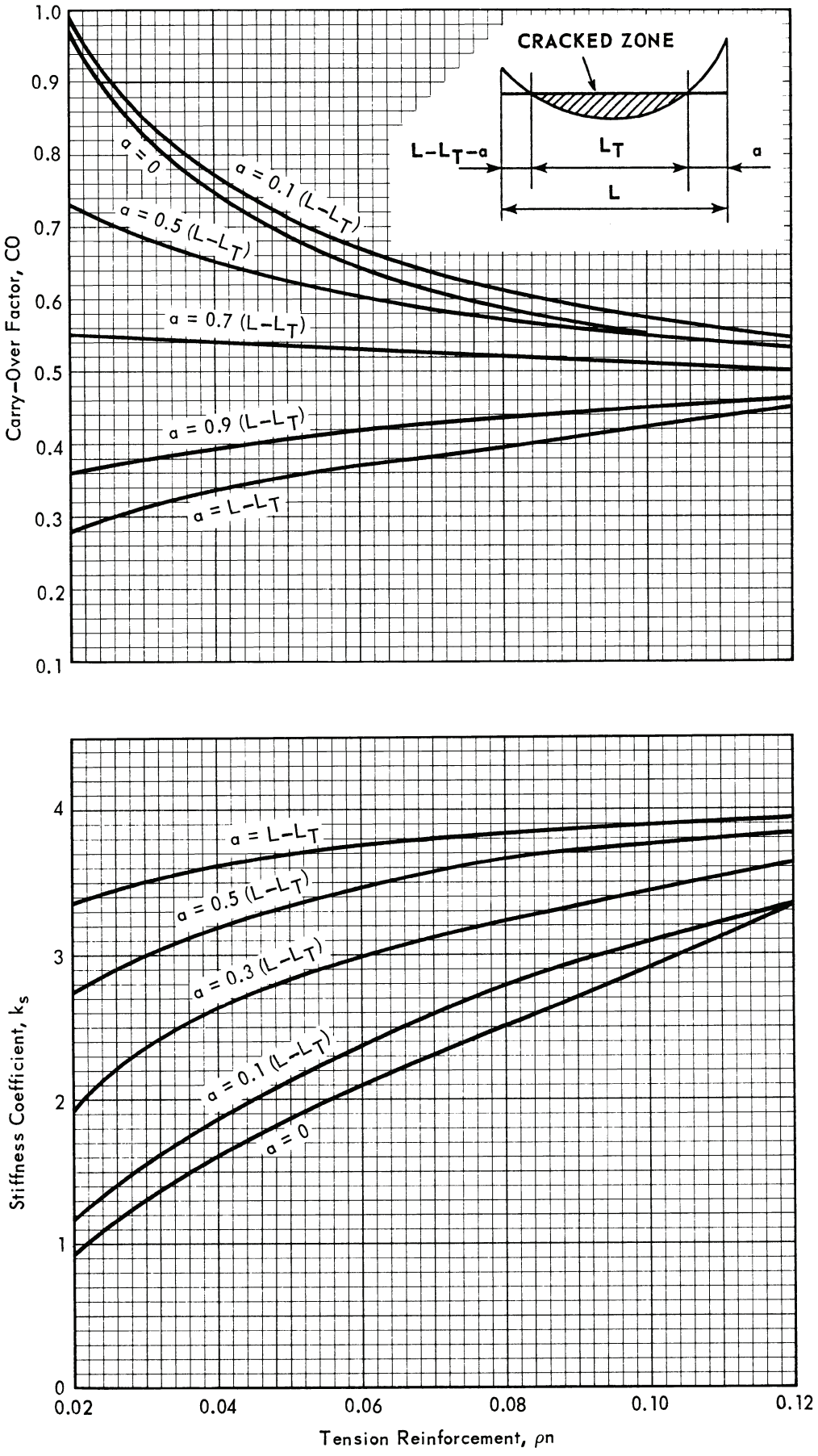

Fig. 3.9—Interior-cracked beam, k_s *and* CO *for* $L_T = 0.4L$.

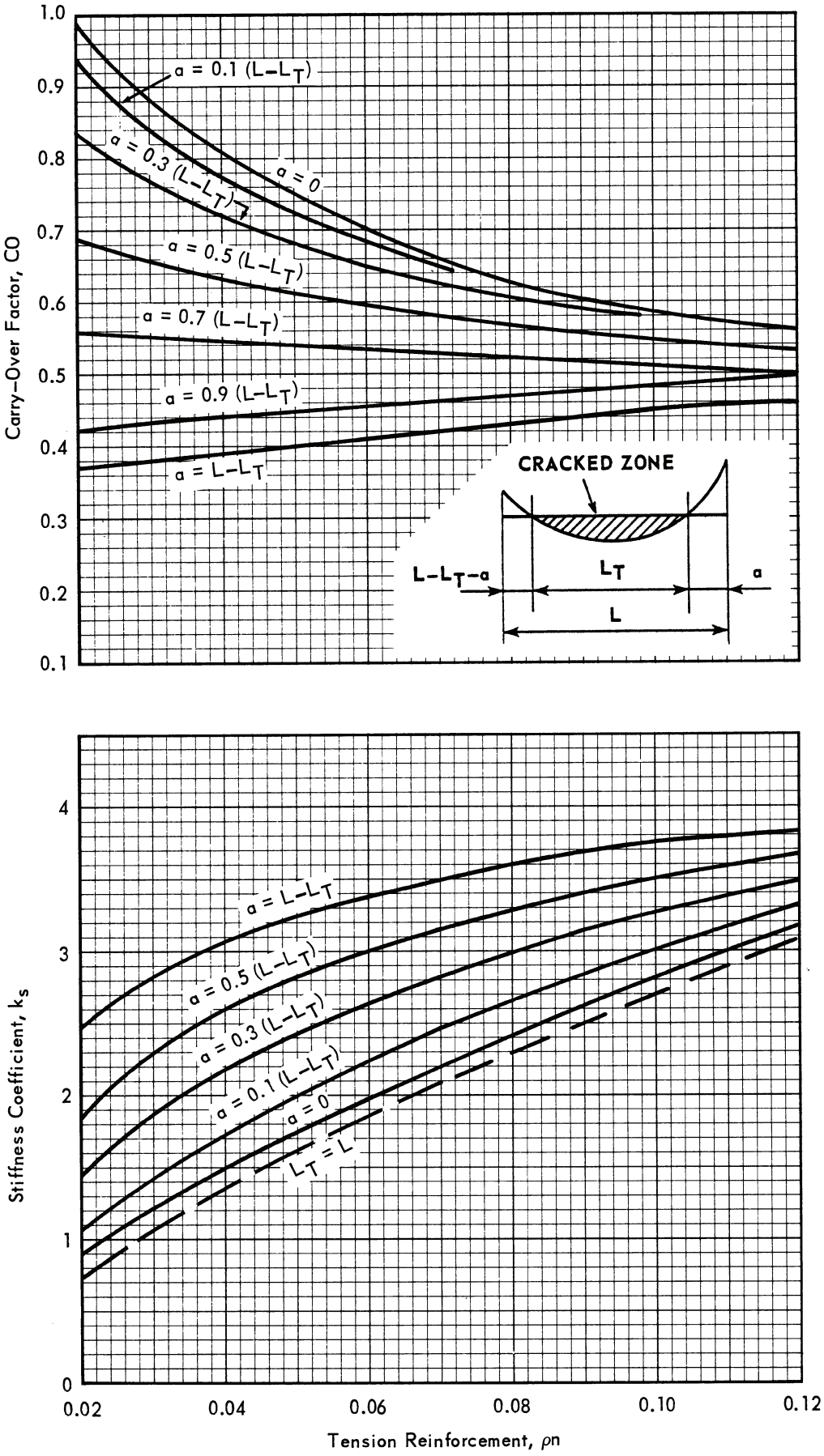

Fig. 3.10—Interior-cracked beam, k_s *and* CO *for* $L_T = 0.6L$.

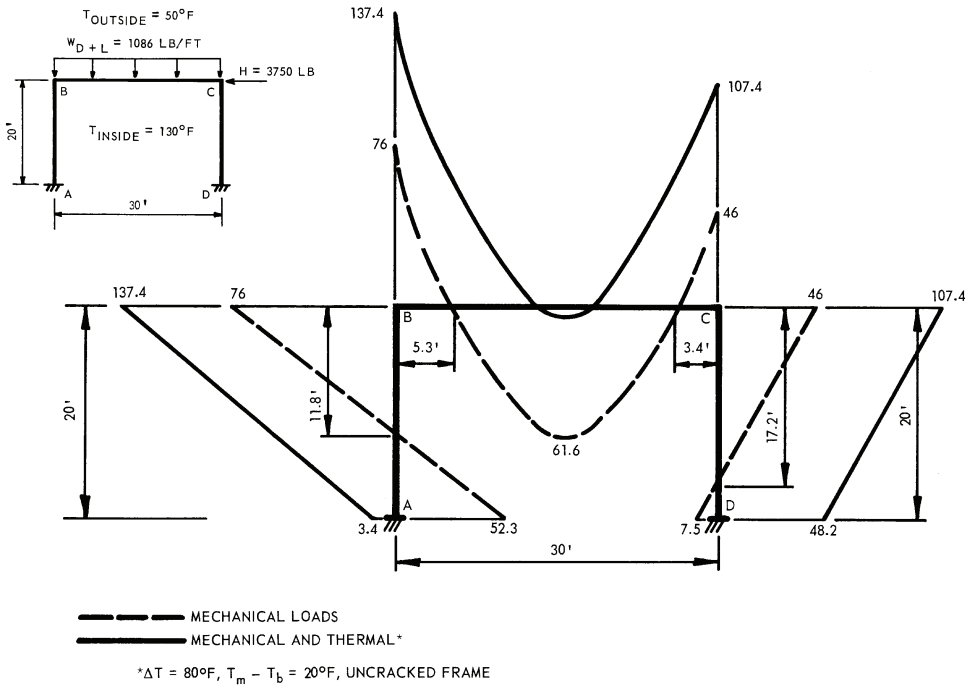

Fig. 3.11—Uncracked frame moments (ft-kips).

The reinforcement in the frame consists of two No. 8 bars at each face in all components. This results in $\rho = A_s/bd = (2 \times 0.79)/12(24 - 3) = 1.58/(12 \times 21) = 0.0063$ and $\rho n = 9.3(0.0063) = 0.059$. $\omega = \rho f_y/f'_c = 0.0063(60/3) = 0.126$; and $K_u = f'_c\,\omega(1 - 0.59\omega) = 3000 \times 0.126(1 - 0.59 \times 0.126) = 378 \times 0.92566 = 349.8$. The section capacity is $M_u = \phi K_u F = (0.9)(349.8) \times (12)(21)^2/12{,}000 = 138.8$ ft-kips.

Mechanical loads—An analysis of the uncracked frame results in the component moments (ft-kips) as follows. Moments acting counterclockwise on a component are denoted as positive. These values were obtained by moment distribution, and moments due to E_{ss} include the effect of frame sidesway.

	Moment (ft-kips)
AB:	–52.3
BA:	–76.0
BC:	+76.0
CB:	–46.0
CD:	+46.0
DC:	+7.5

These are shown in Fig. 3.11.

The maximum mechanical load moment of 76 ft-kips is less than the section capacity of 138.8 ft-kips. Therefore, the frame is adequate for mechanical loads.

Thermal effects ($\Delta T = 80$ °F and $T_m - T_b = 20$ °F)

The $\Delta T = 80$ °F having hot interior and cold exterior is expected to produce thermal stresses that are tensile on the exterior faces of all components. These stresses will add to the existing exterior face tensile stresses due to the mechanical loads. Hence, the L_T and a values are arrived at from the mechanical load moment diagram in Fig. 3.11.

Component	End	L_T/L, ft/ft	a/L_T, ft/ft
AB	A	11.8/20 = 0.59	0
AB	B	0.59	1
BC	B	(5.3 + 3.4)/30 = 0.29	5.3/8.7 = 0.61
BC	C	0.29	3.4/8.7 = 0.39
CD	C	17.2/20 = 0.86	1
CD	D	0.86	0

All components are the end-cracked type. Figures 3.4 through 3.6 are used to obtain the coefficients k_s and CO, which are shown in Table 3.1.

The expressions from Section 3.4 for fixed-end moment (FEM) are evaluated as

$$1.\ \Delta T\ \text{FEM} = \frac{E_c \alpha \Delta T b t^2 k_s}{12}\frac{}{2}(1 - CO)$$

$$= \frac{(3.12 \times 10^6)(5 \times 10^{-6})(80)(12)(24)^2 k_s}{12}\frac{}{2}(1 - CO)$$

ΔT FEM $= 59.9k_s(1 - CO)/2$ ft-kips

$$2.\ T_m - T_b\ \text{FEM} = \frac{E_c I_g}{L^2}(\Delta)(k_s)(1 + CO)$$

$$= \frac{3.12 \times 10^6 (24)^3}{(20 \times 12)^2}(\Delta)(k_s)(1 + CO)$$

$T_m - T_b$ FEM $= 62.4(\Delta)(k_s)(1 - CO)$ ft-kips

3. Δ = total unrestrained change of length of component BC

Table 3.1—Cracked frame coefficients and thermal moments on components

Component	End	L_T/L	a/L_T	k_s	CO	K_y/L	DF	Thermal FEMs, ft-kips			Distributed thermal moments,* ft-kips	Distributed thermal moments and mechanical moments, ft-kips
								ΔT-80 FEM	$T_m - T_b = 20$ FEM	Total FEM		
AB	A	0.59	0	3.40	0.41	0.17	1.0	+60.1	–4.79	+55.31	+36.0	–16.3
AB	B	0.59	1	2.00	0.70	0.10	0.56	–17.97	–3.39	–21.36	–39.9	–115.9
BC	B	0.29	0.61	2.40	0.43	0.08	0.44	+41.7	0	+41.7	+39.9	+115.9
BC	C	0.29	0.39	2.65	0.38	0.088	0.48	–49.2	0	–49.2	–37.0	–83.0
CD	C	0.86	1	1.90	0.57	0.095	0.52	+24.5	+3.72	+28.2	+37.0	+83.0
CD	D	0.86	0	2.39	0.47	0.120	1.0	–37.9	+4.38	–33.5	–33.2	–25.7

*Corrected for sidesway.
Notes: $DFi = (k_{si}E_iI_{gi}/L_i)/(\Sigma k_{si}E_iI_{gi}/L_i)$; symbols with component i are indicated with subscript i.

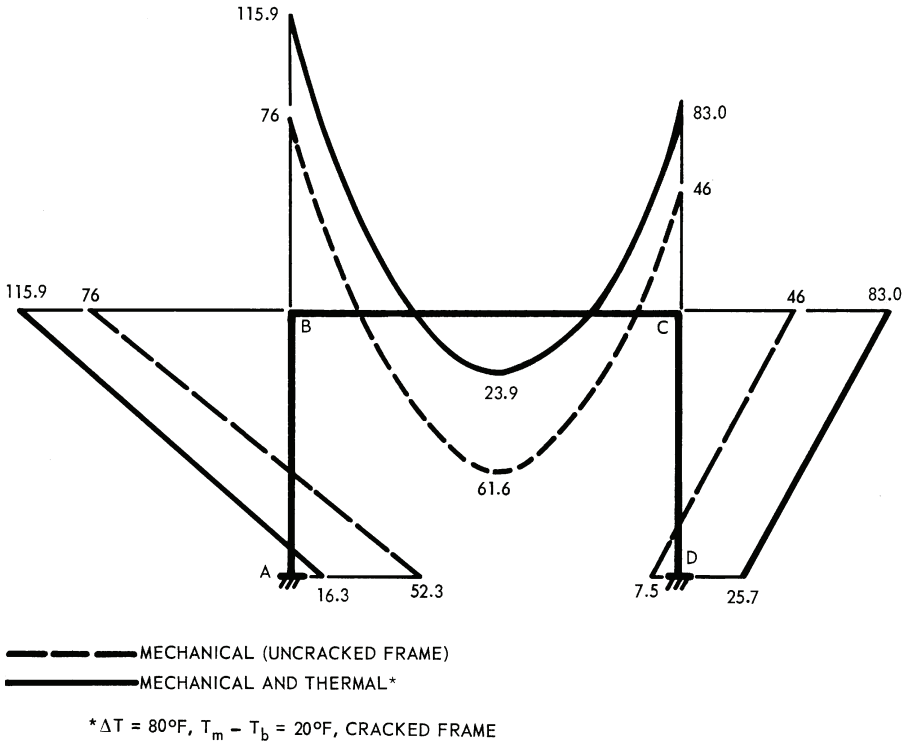

Fig. 3.12—Final frame moments (ft-kips).

$= \alpha(T_m - T_b)L$

$\Delta = (5 \times 10^{-6})(20)(30 \times 12)$

$\Delta = 0.036$ in.

Distribute 0.036 in. to Ends B and C of Components AB and CD, respectively, in inverse proportion to the shear stiffness at these ends.

Shear stiffness at B

$$= \frac{E_cI_g}{L^3}[k_{sA}(1 + CO_A) + k_{sB}(1 + CO_B)]$$

$$= \frac{E_cI_g}{L^3}[3.4(1.41) + 2.00(1.70)]$$

$$= \frac{E_cI_g}{L^3}(8.19)$$

Shear stiffness at C

$$= \frac{E_cI_g}{L^3}[k_{sC}(1 + CO_C) + k_{sD}(1 + CO_D)]$$

$$= \frac{E_cI_g}{L^3}[1.90(1.57) + 2.38(1.47)]$$

$$= \frac{E_cI_g}{L^3}(6.48)$$

Sum of shear stiffness at B and C $= \frac{E_cI_g}{L^3}(14.67)$

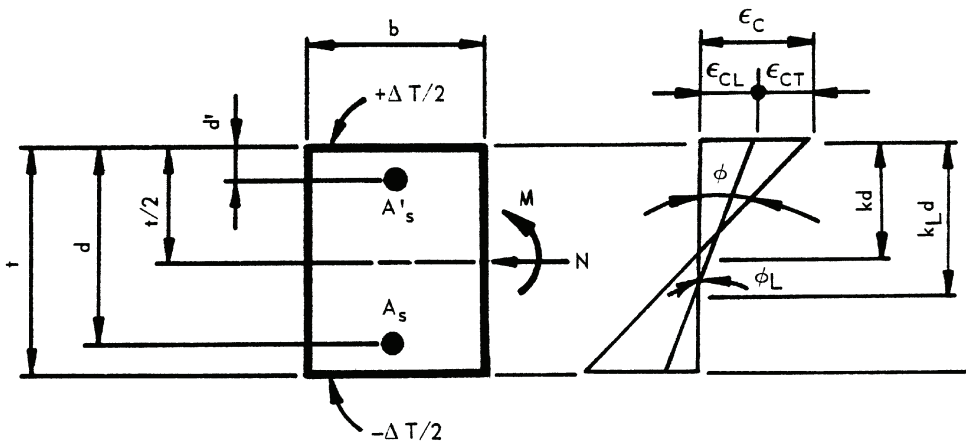

Fig. 4.1—Section under M, N, *Δ*T.

Δ_B = 0.036 in. (6.48/14.67) = 0.036 × 0.44 = 0.016 in.

Δ_C = 0.036 in. (8.19/14.67) = 0.036 × 0.56 = 0.020 in.

To demonstrate the effect of cracking on the thermal moments, the fixed-end thermal moments for the uncracked frame are obtained from the final expressions in 1 and 2 using k_s = 4, CO = 1/2, and $\Delta = (1/2)\alpha(T_m - T_b)L$, with L being the length of Component BC. A moment distribution is performed, and the resulting distributed moments are added to the mechanical moments. The combined moments are shown in Fig. 3.11 for comparison with the cracked frame moments.

The fixed-end thermal moments for the cracked frame are obtained using the aforementioned values for Δ_B and Δ_C and by referring to Table 3.1 for k_s and CO. These fixed-end moments and the resulting distributed thermal moments are given in Table 3.1. The distributed thermal moments include the effect of sidesway, which occurs because the frame is unsymmetrically cracked.

Combined loads—The final frame moments are shown in Table 3.1 and Fig. 3.12. These can be compared with Fig. 3.11 to see the effect of the cracking reduction of thermal moments.

Although not shown, the component axial forces were evaluated to confirm that section cracking still corresponds to the pure bending condition of Assumption 3. Recall that *e*/*d* should be at least 0.5 for this condition. For Components AB and CD, the axial forces result primarily from the mechanical loads and are compressive. For Component BC, the axial force is compressive and includes the compression due to the 20 ºF increase on the component.

CHAPTER 4—AXISYMMETRIC STRUCTURES

4.1—Scope

Axisymmetric structures include shells of revolution such as shield buildings or, depending on the particular geometry, primary and secondary shield walls. In the structural analysis, the structure is considered to be uncracked for all mechanical loads and for part of the thermal effects. The thermal effect is assumed to be represented by a temperature that is distributed linearly through the wall of the structure. The linear temperature distribution is separated into a gradient ΔT and into a uniform temperature change $T_m - T_b$.

Generally, for most axisymmetric structures, a uniform temperature change ($T_m - T_b$) produces significant internal section forces (moment included) only at the externally restrained boundaries of the structure where movement due to thermal change is prevented, or in regions where $T_m - T_b$ varies fairly rapidly along the structure. The magnitude and extent of these discontinuity forces depend on the specific geometry of the structure and on the external restraint provided. If cracking occurs in this region, a prediction of the cracking reduction of the discontinuity forces is attainable through a re-analysis using cracked section structural properties. A discussion of such an analysis is not within the scope of this report. Therefore, forces resulting from an analysis for the $T_m - T_b$ part of the thermal effect are considered to be included with corresponding factored mechanical forces. These combined axial forces and moments are denoted as N and M.

The gradient ΔT produces internal section forces (moment included) at externally restrained boundaries, and also away from these discontinuities. At discontinuities, the most significant internal force is usually the moment, primarily resulting from the internal restraint rather than the external boundary restraint. Away from discontinuities, the only significant forces due to T are thermal moments caused by the internal restraint provided by the axisymmetric geometry of the structure. The cracking reduction of thermal moments that result from internal restraint is the subject of this chapter.

Due to the axisymmetric geometry of the subject structures, the free thermal curvature change $\alpha\Delta T/t$ is fully restrained. This restraint produces a corresponding thermal moment whose magnitude depends on the extent of cracking the section experiences. This in turn depends on ΔT, the other section forces N and M, and the section properties (Fig. 4.1). With the ratio M/N denoted as e, referenced to the section centerline, and the distance from the concrete compression face to the tension reinforcement denoted as d, two cases of e/d are identified in Sections 4.2 and 4.3.

The results in Sections 4.2 and 4.3 include the effect of compression reinforcement. For this reinforcement, a modular

ratio of $2n$ (Ferguson 1965) is used for purposes of simplifying the determination of the cracked section thermal moment. Although not all the loads that comprise the section forces N and M will necessarily be long-term, the selection of $2n$ for compression reinforcement is consistent with design practice.

The results in Sections 4.2 and 4.3 are based on a linear stress-strain relationship for the compressive concrete. The basis of this assumption was discussed in Section 3.2. From this discussion, the cracked section thermal moments can be considered to represent upper-bound values when compared with those that would result from a nonlinear stress-strain concrete relationship. Nevertheless, the thermal moments herein do offer a reduction from their uncracked values. The extent of this reduction is shown in Fig. 4.2 through 4.8.

4.2—$|e/d| \geq 0.7$ for compressive N and tensile N

For this range of e/d, a parametric study based on the results of Section 4.3 indicates that the cracked thermal moment $M_{\Delta T}$ is not strongly influenced by the axial force as expressed by the ratio $N/(bdE_c\alpha\Delta T)$. A practical range of $N/(bdE_c\alpha\Delta T)$ from 0 to ±300 was used in this study. Therefore, for ranges of e/d and $N/(bdE_c\alpha\Delta T)$ specified herein, $M_{\Delta T}$ can be calculated from the neutral axis location corresponding to $N = 0$.

The $|e/d|$ lower limit of 0.70 is conservative for tensile N and higher ρn values. Actual $|e/d|$ lower limits for tensile N are given in Fig. 4.9. As long as the actual $|e/d|$ value for tensile N exceeds this lower-limit curve, the thermal moments given in this section are applicable.

For doubly reinforced rectangular sections, the cracked section neutral axis is kd. For $N = 0$

$$k = \sqrt{(2\rho' n + \rho n)^2 + 2[2\rho' n(d'/d) + \rho n]} - (2\rho' n + \rho n) \qquad (4\text{-}1)$$

in which $\rho' = A_s'/bd$, $\rho = A_s/bd$, and $n = E_s/E_c$. Also, d' is the distance from the concrete compression face to the compression reinforcement A_s'. A modular ratio of $2n$ is used for the compression reinforcement.

The corresponding thermal moment for a section in which $t = (1.1)d$ is

$$M_{\Delta T} = E_c \frac{\alpha\Delta T b d^2}{1-\nu}\{-0.152k^3 + 1.818\rho' n[(d'/d) - k](d'/d) + 0.909\rho n(1-k)\} \qquad (4\text{-}2)$$

The expression for $M_{\Delta T}$ given by Eq. (4-2) is obtained from the results of Section 4.3 in the following manner. For sections in which $|e/d| \geq 0.7$, the location of the neutral axis does not change under the application of ΔT, and this results in $k_L = k$. This substitution for k_L is made in Eq. (4-7) and (4-9). The resulting expression for f_c given by Eq. (4-7) is used in Eq. (4-11). $M_{\Delta T}$ is then obtained by subtraction of Eq. (4-9) from Eq. (4-11).

For singly reinforced rectangular sections and $N = 0$

$$k = \sqrt{(\rho n)^2 + 2\rho n} - \rho n \qquad (4\text{-}3)$$

and the corresponding thermal moment is

$$M_{\Delta T} = \frac{E_c\alpha\Delta T b d^3(jk^2)}{2t(1-\nu)} \qquad (4\text{-}4)$$

where $j = 1 - k/3$.

Equation (4-2) for $M_{\Delta T}$ for a doubly reinforced section reduces to $M_{\Delta T}$ for a singly reinforced section (Eq. (4-4)), with the substitution of $(1.1)d$ for t in Eq. (4-4), and 0 for $\rho' n$ in Eq. (4-2). In addition, the substitution of $k^2/2$ for $\rho' n(1-k)$ in Eq. (4-2) must be made.

The thermal moments given by Eq. (4-2) and (4-4) are presented in Fig. 4.2 for the special case: $t = (1.1)d$ for both sections, and $\rho' n = \rho n$ and $d'/d = 0.10$ for the doubly reinforced section. For values of ρ' less than ρ, linear interpolation between the two curves should yield sufficiently accurate results. From Fig. 4.2, it is seen that the cracked section thermal moment is substantially reduced from its uncracked value.

The thermal moment $M_{\Delta T}$ occurs at the centerline of the section. $M_{\Delta T}$ should be multiplied by its code-specified load factor before it is added to the moment M.

4.3—General e/d

Depending on e/d, the extent of section cracking and the thermal moment may be significantly affected by the actual values of N and M. A theory for the investigation of a doubly reinforced rectangular section is presented. The Poisson's effect increases the section thermal moment due to ΔT by an amount $1/(1-\nu)$. Although this effect is not shown in the following derivations, it is included in the final results (Fig. 4.2 through 4.8).

It is assumed for the section that the final curvature change ϕ is equal to ϕ_L, the curvature change due to N and M plus ϕ_T, the curvature change due to Δ_T. ϕ_L and ϕ_T are additive when the cold face of the section corresponds to the tension face under M. Therefore

$$\phi = \phi_L + \phi_T \qquad (4\text{-}5)$$

The curvatures before and after the application of ϕ_T are shown in Fig. 4.1.

The thermal curvature change ϕ_T is

$$\phi_T = \alpha\Delta T/t$$

where ΔT is always taken as positive.

Using this and $\varepsilon_c = \phi kd$ and $\varepsilon_{cL} = \phi_L k_L d$ in Eq. (4-5) gives

$$\varepsilon_c/kd = \varepsilon_{cL}/k_L d + \alpha\Delta T/t \qquad (4\text{-}6)$$

For the case where the concrete stress is a linear function of strain, Eq. (4-6) becomes

$$f_c/(E_c kd) = f_{cL}/(E_c k_L D) + \alpha\Delta T/t$$

or

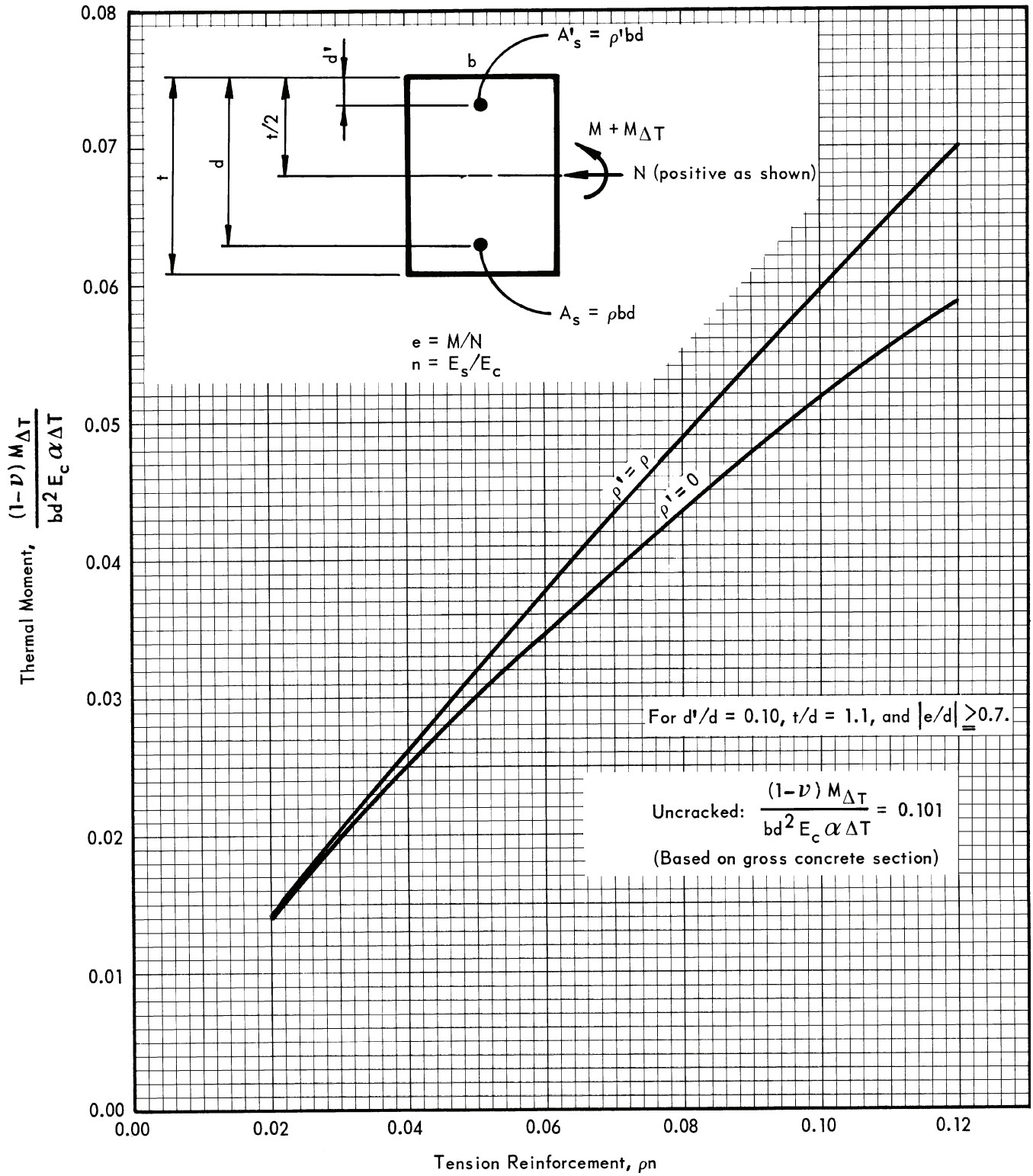

Fig. 4.2—Cracked section thermal moment for |e/d| ≥ 0.70.

$$f_c = [f_{cL}/(E_c k_L d) + \alpha\Delta T/t]E_c kd \quad (4\text{-}7)$$

To maintain equilibrium of the section both before and after the application of ΔT, the following conditions occur:

Before T

1. The internal axial force N is equal to the resultant of the stresses produced by N and M

$$N = 1/2 f_{cL} b k_L d + 2\rho' nbdf_{cL}[(k_L - d'/d)/k_L] + \rho nbdf_{cL}[(k_L - 1)/k_L] \quad (4\text{-}8)$$

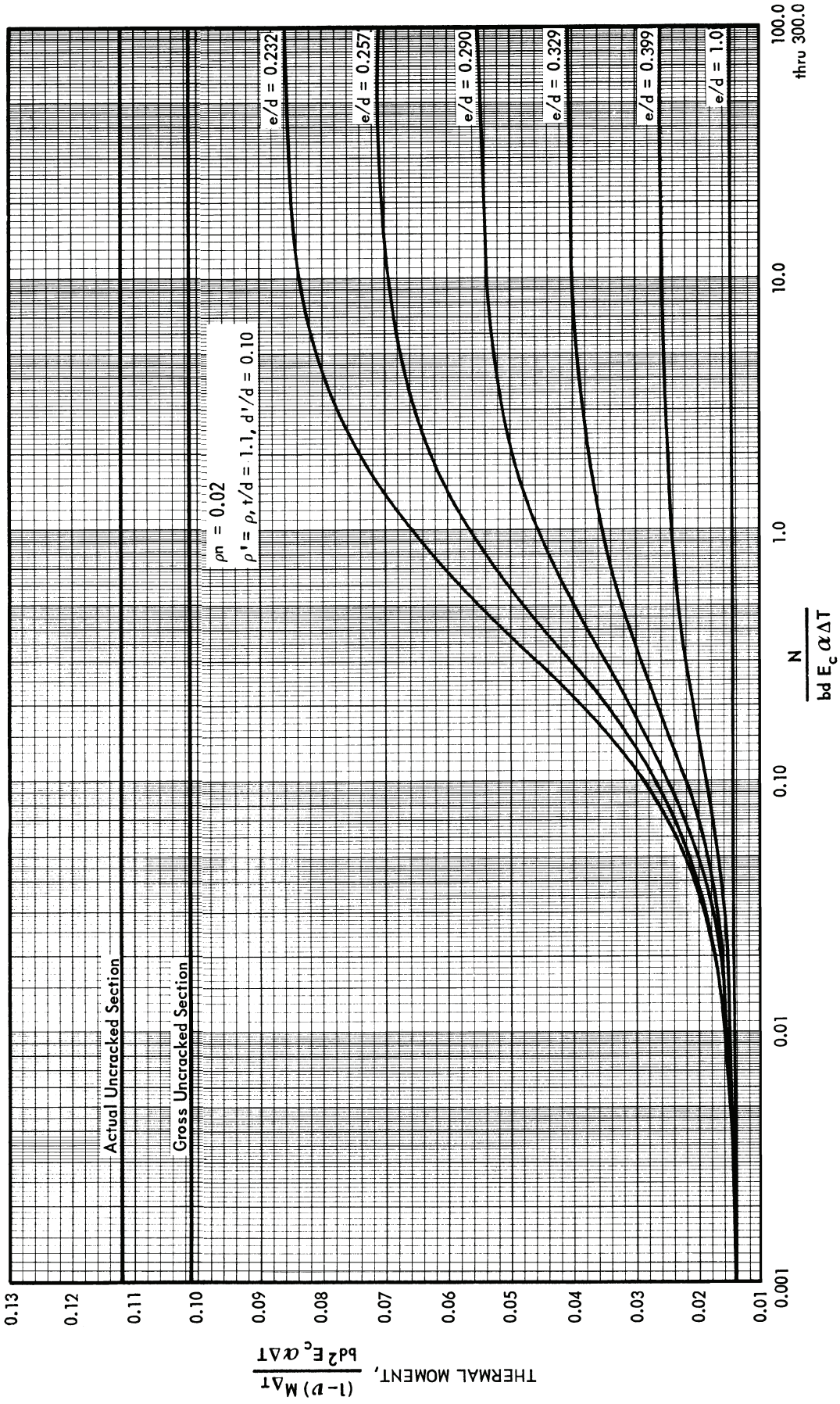

Fig. 4.3—Thermal moments for compressive N, ρn = *0.02.*

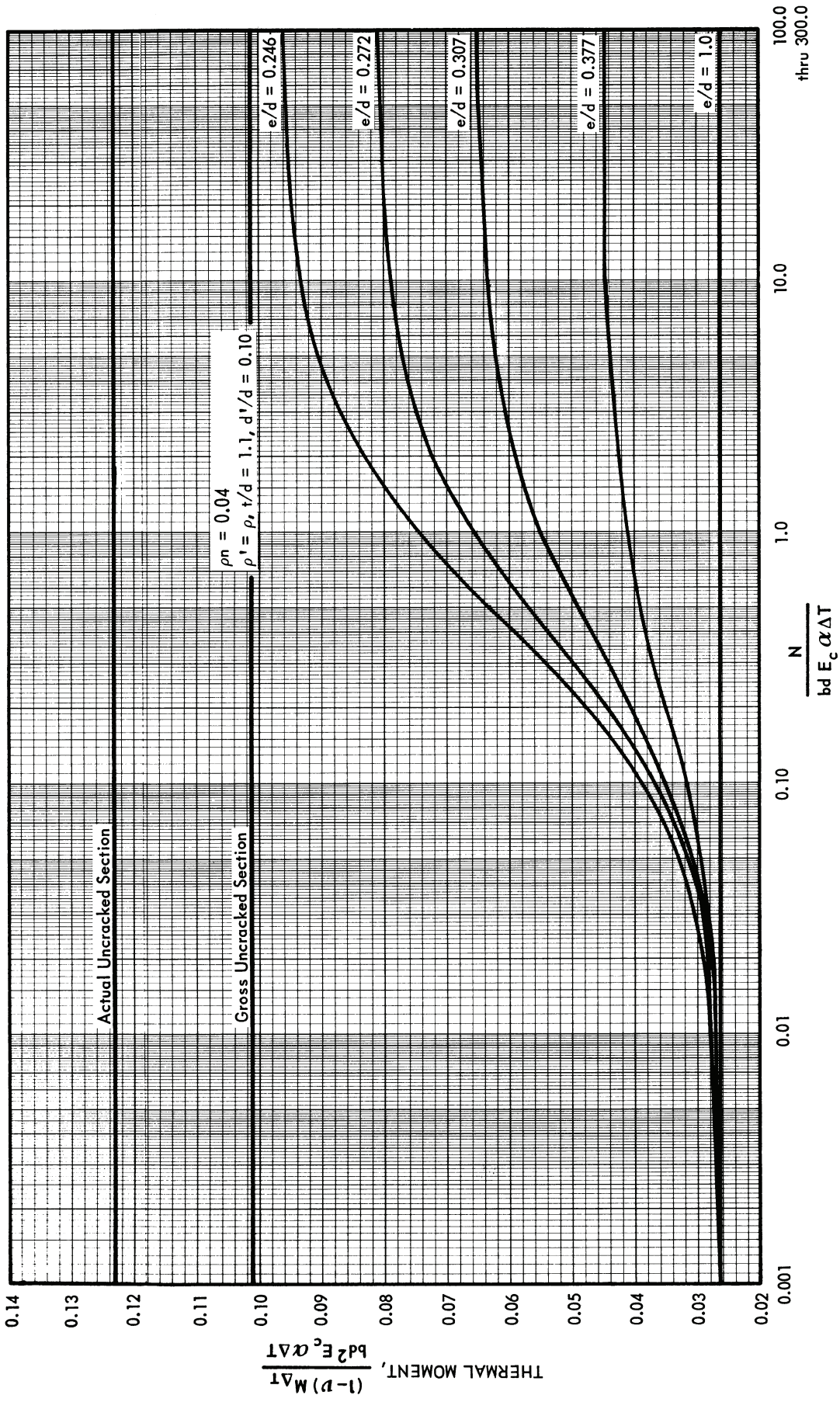

Fig. 4.4—Thermal moments for compressive N, ρn = *0.04.*

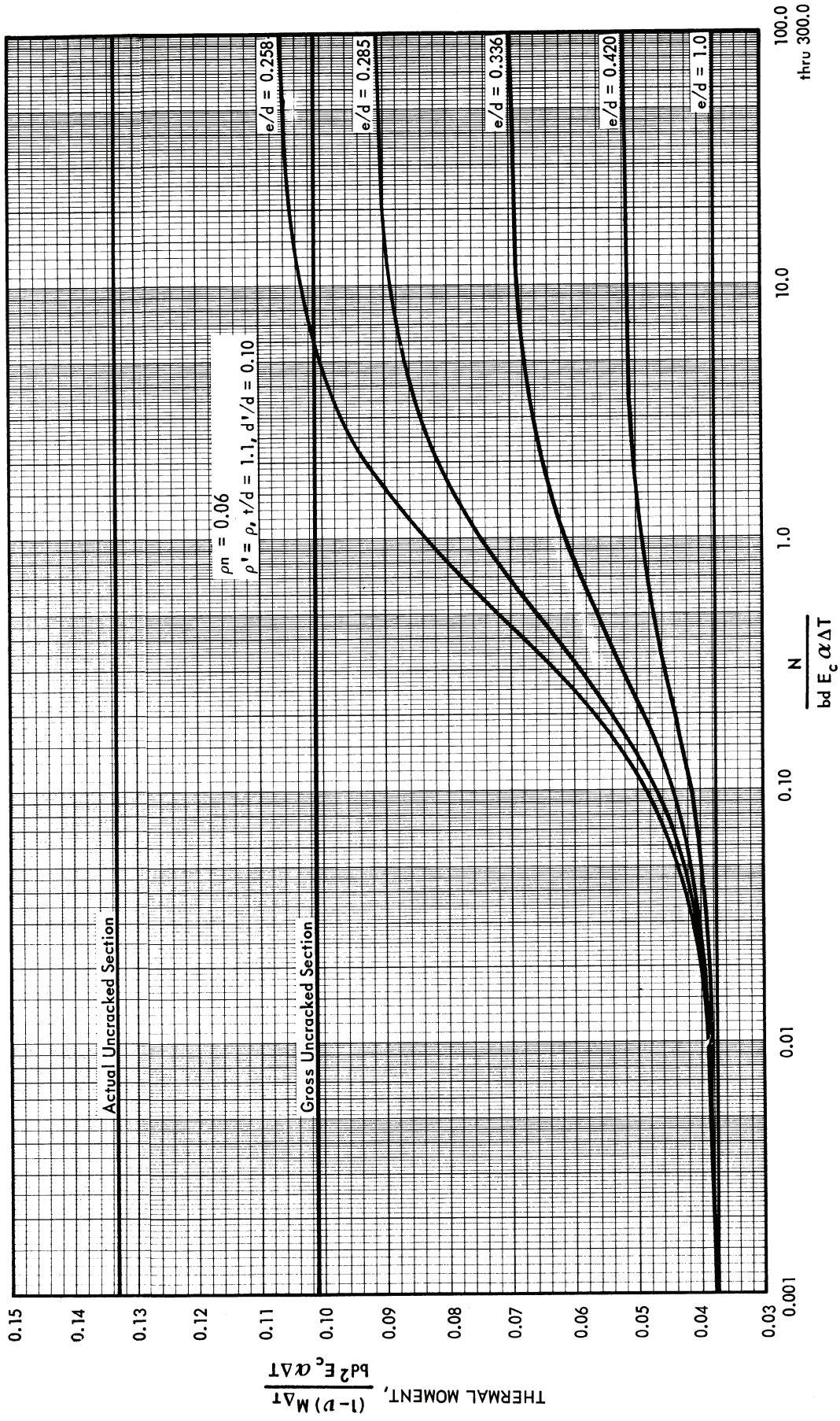

Fig. 4.5—Thermal moments for compressive N, ρn = *0.06.*

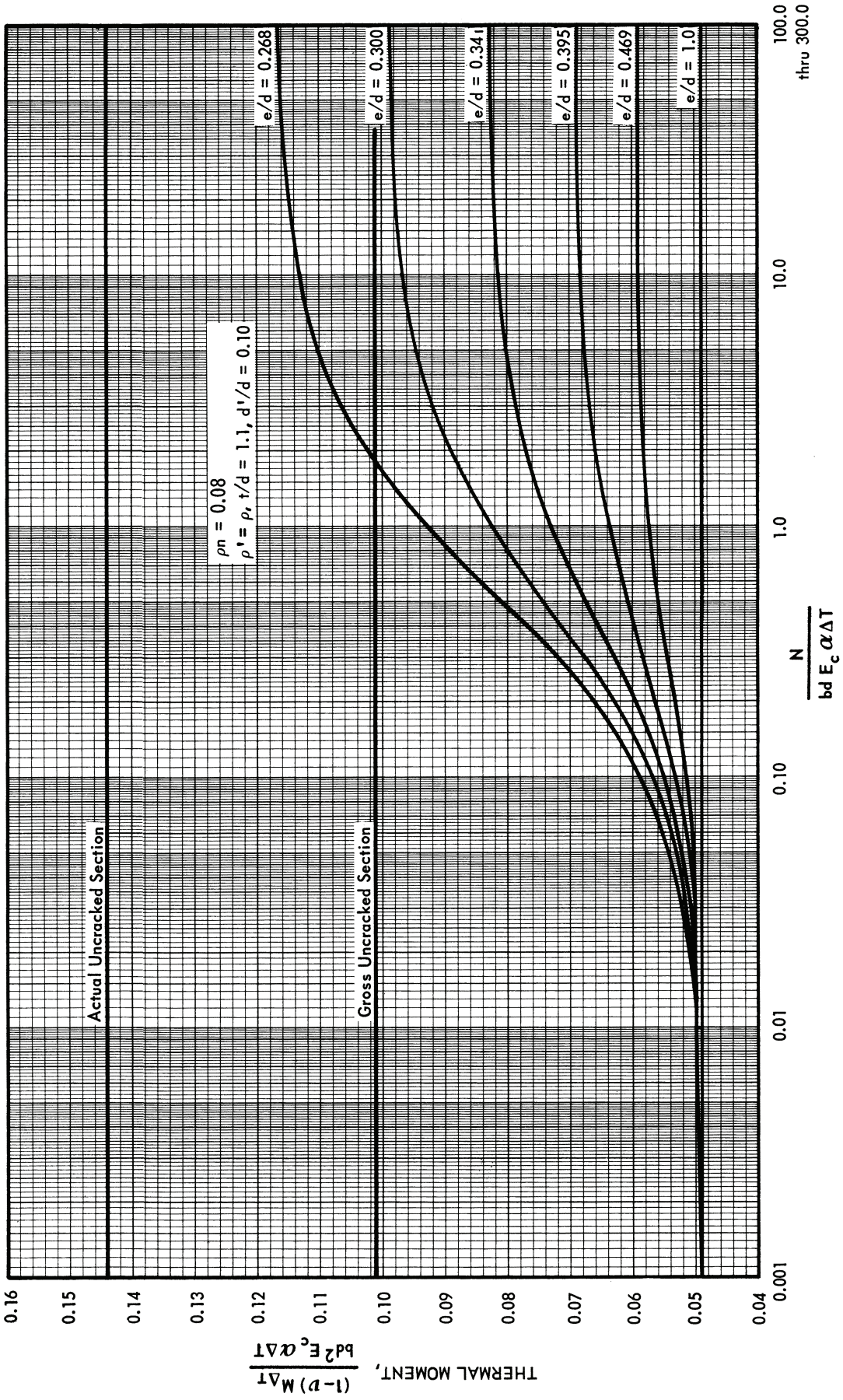

Fig. 4.6—Thermal moments for compressive N, ρn = *0.08.*

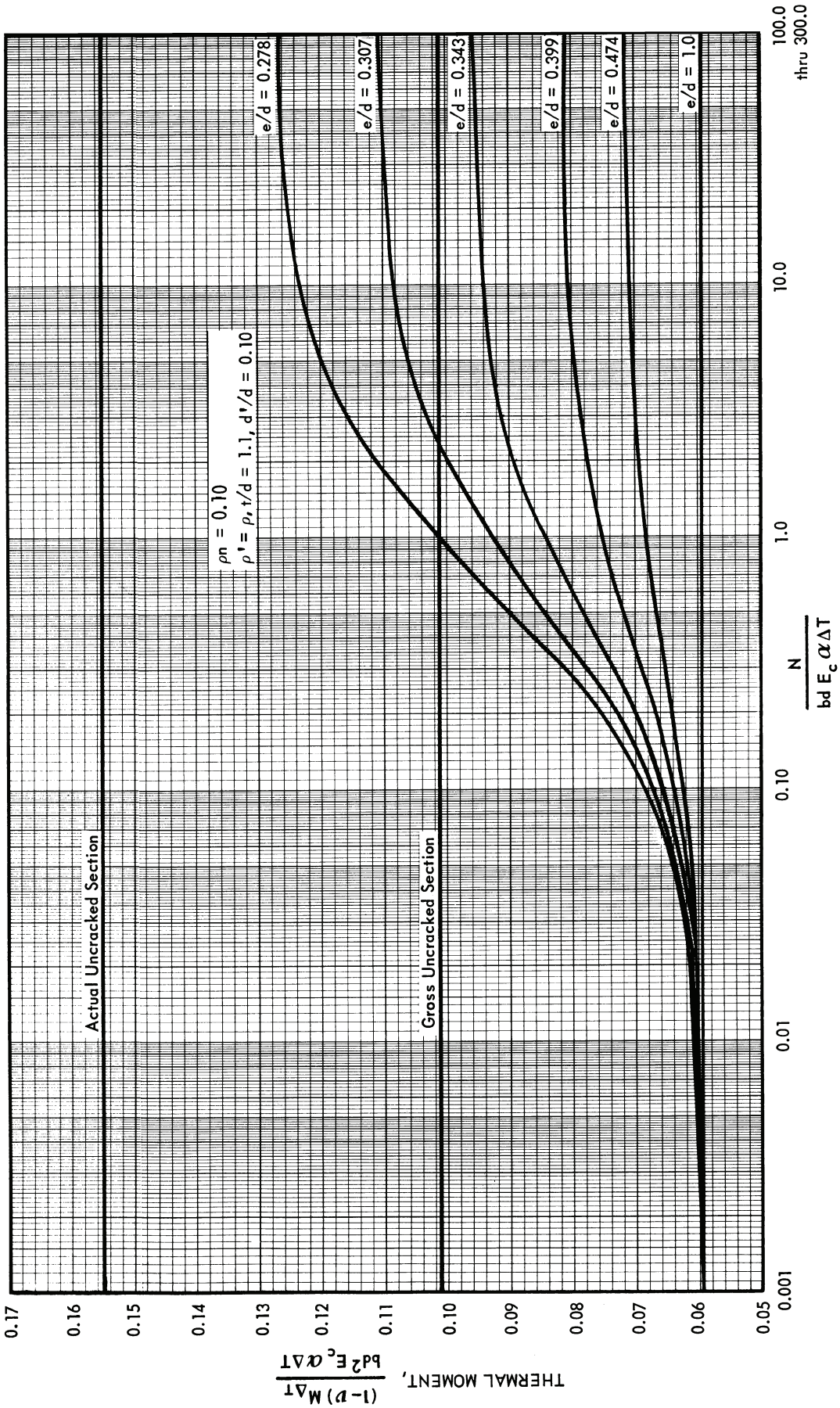

Fig. 4.7—Thermal moments for compressive N, ρn = *0.10.*

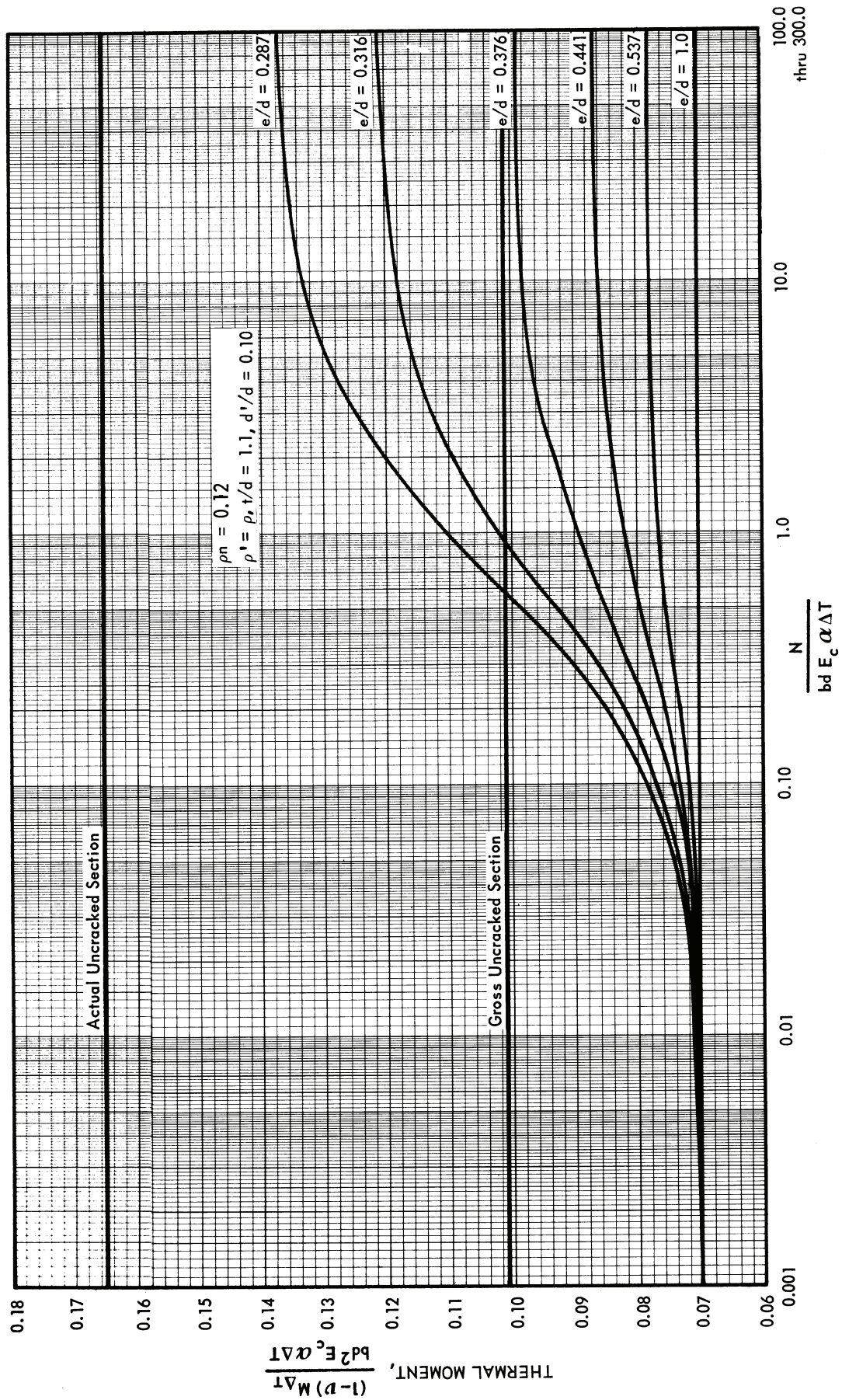

Fig. 4.8—Thermal moments for compressive N, ρn = *0.12.*

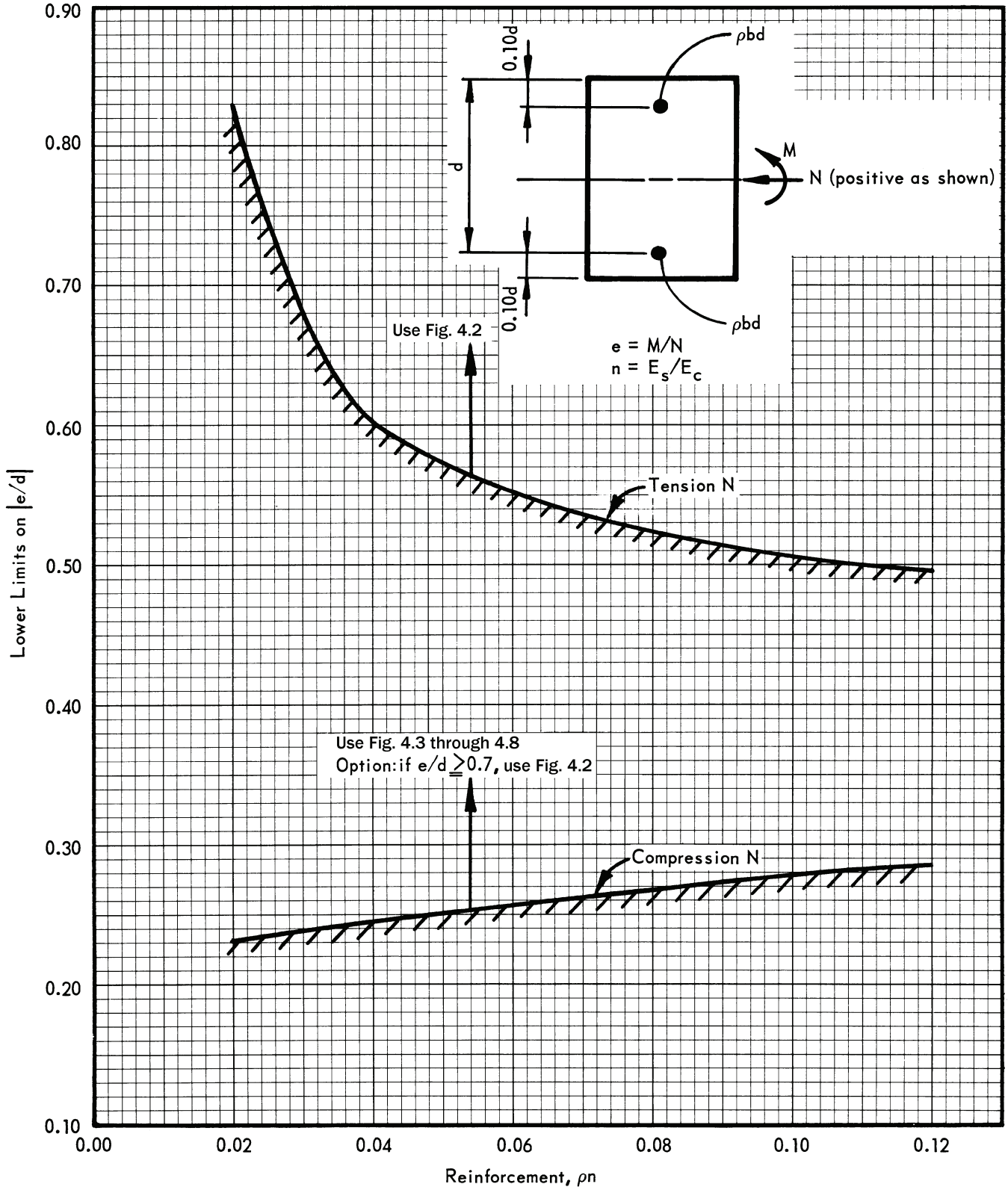

Fig. 4.9—e/d *limits.*

2. The internal moment M is equal to the internal moment of the stresses (about the section centerline) produced by N and M.

$$M = 1/2 f_{cL} b k_L d(t/2 - k_L d/3) + 2\rho' nbdf_{cL} \times [(k_L - d'/d)/k_L] \quad (4\text{-}9)$$

$$[(t/2) - d'] + \rho nbdf_{cL} \times [(1 - k_L)/k_L][d - (t/2)]$$

After ΔT

1. The internal axial force N is equal to the resultant of the stresses produced by N, M, and ΔT

$$N = 1/2 f_c bkd + 2\rho'[(k - d'/d)/k] + \rho nbdf_c[(k - 1)/k] \quad (4\text{-}10)$$

2. There exists an internal centerline moment (moment about centerline for internal forces) $\overline{M}$ of the stresses produced by N, M, and ΔT.

$$\overline{M} = 1/2 f_c bkd[(t/2) - (kd/3)] + 2\rho' nbdf_c[(k - d'/d)/k] \quad (4\text{-}11)$$

$$\times [(t/2) - d'] + qnbdf_c[(k - 1)/k][d - (t/2)]$$

3. The internal thermal moment $M_{\Delta T}$ at the section centerline is equal to $\overline{M} - M$.

In Eq. (4-8) through (4-11), the tension and compression reinforcement have been expressed as $\rho = A_s/bd$ and $\rho' = A_s'/bd$, respectively. A modular ratio of $2n$ has been used for the compression reinforcement. Also, the reinforcement stresses have been expressed in terms of the concrete stress.

From Eq. (4-8), f_{cL} can be expressed in terms of N, k_L, and the section properties. The use of this in Eq. (4-7) allows f_c to be written in terms of N, k_L, k, $E_c\alpha\Delta T$, and the section properties. Substitution of this expression for f_c into Eq. (4-10) results in a quadratic equation in k that is solved in terms of the section properties, k_L, and the quantity $N/bdE_c\alpha\Delta T$. By dividing Eq. (4-9) by Eq. (4-8), however, k_L can be written in terms of the section properties and e, where $e = M/N$. Thus, k is determined for a specified section e and $N/bdE_c\alpha\Delta T$. The aforementioned results also allow $M_{\Delta T}$ to be determined from these specified quantities.

The equilibrium equations, appearing as Eq. (4-8) through (4-11), are based on a triangular concrete stress distribution. The two extremes of the stress distribution are at $k_L = 0.10$ and $k_L = 1.0$. The range $1.0 \geq k_L \geq 0.10$ should cover many practical situations not involving prestressed sections. For k_L outside this range, that is, the entire section being under tension ($k_L \geq 0.10$) or compression ($k_L \geq 1.0$), a similar set of equilibrium equations based on a rectangular stress distribution would be required.

Special case

$$\rho' = \rho,\ t/d = 1.1,\ \text{and}\ d'/d = 0.10$$

For this case, cracked section thermal moments were calculated for a ρn range of 0.02 to 0.12 and $N/bdE_c\alpha\Delta T$ ranging within ±300. For the case of compressive N, Fig. 4.3 through 4.8 apply. Alternatively, for compressive N and $e/d \geq 0.7$, Fig. 4.2 may be used with reasonable accuracy. For the case of tensile N, only Fig. 4.2 applies.

As previously discussed, the thermal moments are valid only for $1.0 \geq k_L \geq 0.10$. Associated with these limits are e/d values that are indicated in Fig. 4.9.

Also presented in Fig. 4.3 through 4.8 are the uncracked thermal moments based on both gross section (neglecting reinforcement) and actual section (including concrete and reinforcement). It is seen that the cracked section thermal moments are always less than the uncracked thermal moments obtained for the actual section. For the combination of higher ρn values and lower e/d values, however, the cracked section thermal moments exceed the uncracked thermal moments based on a gross concrete section. This is due to the fact that the increase in section flexural stiffness (EI) due to inclusion of the reinforcement is greater than the loss of section flexural stiffness that results from the relatively minor cracking associated with the low e/d value. The net effect is to give a larger actual cracked section stiffness than that obtained for the gross uncracked concrete section alone.

If the designer finds these cracked section thermal moments to be unacceptably high, a potential reduction may be available through the use of an approach incorporating a nonlinear representation of the concrete stress-strain behavior. Such an approach is described in Fu and Daye (1991), Gurfinkel (1972), and Kohli and Gurbuz (1976).

4.4—Design examples

4.4.1 ***Example 1:*** *Compressive* N *and* |e/d| > 0.70, $\rho' = \rho$ $b = 12$ in., $t = 36$ in., $d = 32.7$ in., $d' = 3.3$ in., $A_s' = 2$ in.^{2}, $A_s = 3$ in.^{2}, $E_s = 29 \times 10^6$ psi, $E_c = 4 \times 10^6$ psi, $\nu = 0.2$, $N = 50$ kips compression, $M = 100$ ft-kips, $\Delta T = 80$ °F

$n = E_s/E_c = 29/4 = 7.25$, $e = M/N = 100/50 = 2$ ft $= 24$ in., $\rho' = 2/12 \times 36 = 0.0046$, $\rho' n = 0.0046 \times 7.25 = 0.033$, $\rho = 3/12 \times 36 = 0.0069$, $\rho n = 0.0069 \times 7.25 = 0.050$

Cracked thermal moment $M_{\Delta T}$

e/d ratio: $e/d = 24/32.7 = 0.733 > 0.70$; therefore, Section 4.2 results should be used.

Because $t/d = 1.1$ and $d'/d = 0.10$, Fig. 4.2 should be used. Because $\rho' \neq \rho$, however, interpolate between the two curves.

From Fig. 4.2 for $\rho n = 0.050$, $(1 - \nu)M_{\Delta T}/(bd^2E_c\alpha\Delta T)$ should be read as

$$0.0303 \text{ for } \rho' = 0$$

$$0.0320 \text{ for } \rho' = \rho$$

Interpolate for $\rho' = 0.0046$

$$(1 - \nu)M_{\Delta T}/(bd^2E_c\alpha\Delta T) = 0.0303 + (0.0320 - 0.0303)(0.0045/0.0069) = 0.0314$$

$$(1 - \nu)M_{\Delta T} = 0.0314(12)(32.7)^2(4 \times 10^6) \times (5.5 \times 10^{-6})(80) = 709{,}000 \text{ in.-lb}$$

$M_{\Delta T} = 886{,}000$ in.-lb or 73.9 ft-kips

Check using equations

$$k_{N=0} = \sqrt{(2\rho' n + \rho n)^2 + 2[2\rho' n(d'/d) + \rho n]} - (2\rho' n + \rho n) = [(2 \times 0.033 + 0.050)^2 + 2(2 \times 0.033 \times 0.10 + 0.050)]^{1/2} - (2 \times 0.033 + 0.050) = 0.239$$

$$(1 - \nu)M_{\Delta T}/(bd^2E_c\alpha\Delta T) = -0.152k^3 + 1.818\rho' n(d'/d - k) \times (d'/d) + 0.909\rho n(1 - k) = -0.152(0.239)^3 + 1.818(0.034) \times (0.1 - 0.239)(0.10) + 0.909(0.050) \times (1 - 0.239) = 0.0317$$

$M_{\Delta T} = 73.9(0.0317/0.0314) = 74.6$ ft-kips ≈ 73.9 ft-kips, OK

Table 4.1—Summary of results for Examples 1, 2, 3, and 4

Example	Axial force N, kips	Type	Moment M, ft-kips	Temperature differential ΔT, °F	Compression reinforcement A_s', in.^{2}	Tension reinforcement A_s, in.^{2}	Cracked thermal moment $M_{\Delta T}$, ft-kips	Total moment $(M + M_{\Delta T})$, ft-kips	e/d	Use figure
1	50	Compression	100	80	2	3	73.9	173.9	0.733 > 0.70	Use Fig. 4.2
2	50	Tension	100	80	3	3	75.3	175.3	0.733 > 0.70	Use Fig. 4.2
3	100	Compression	100	80	3	3	95.3	195.3	0.367 < 0.70 0.367 > 0.25	Use Fig. 4.4, 4.5, and 4.9
4	60	Tension	100	80	3	3	75.3	175.3	0.612 < 0.70 0.612 > 0.575	Use Fig. 4.2 and 4.9

Concrete and reinforcement stresses are calculated from a cracked section investigation with $N = 50$ kips compression and $M = 173.9$ ft-kips at section centerline.

4.4.2 ***Example 2:*** *Tensile* N *and* |e/d| > *0.70*, $\rho' = \rho$

$b = 12$ in., $t = 36$ in., $d = 32.7$ in., $d' = 3.3$ in., $A_s' = A_s = 3.0$ in.^{2}, $E_s = 29 \times 10^6$ psi, $E_c = 4 \times 10^6$ psi, $\nu = 0.2$, $N = 50$ kips tension, $M = 100$ ft-kips, and $\Delta T = 80$ °F

$n = 7.25$, $e = 100/–50 = –2$ ft $= –24$ in., $\rho' = \rho = 0.0069$, $\rho' n = \rho n = 0.050$

Cracked thermal moment $M_{\Delta T}$

$e/d = –24/32.7 = –0.733$, $|e/d| = 0.733 > 0.7$; therefore, Fig. 4.2 should be used.

From Fig. 4.2 with $\rho' n = 0.050$ and $\rho' = \rho$ curve,

$$(1 - \nu)M_{\Delta T}/(bd^2E_c\alpha\Delta T) = 0.032$$

$M_{\Delta T} = (1.25)(12)(32.7)^2(4)(5.5)(80)(0.032) = 903{,}000$ in.-lb

$M_{\Delta T} = 75.3$ ft-kips

Concrete and reinforcement stresses are calculated from a cracked section investigation with $N = 50$ kips tension and $M = 175.3$ ft-kips at section centerline.

4.4.3 ***Example 3:*** *Compressive* N *and* |e/d| < 0.70

Same section as Example 2.

$N = 100$ kips compression, $M = 100$ ft-kips, $\Delta T = 80$ °F

$$e = \frac{100 \text{ ft-kips}}{100 \text{ kips}} = 1 \text{ ft} = 12 \text{ in.}$$

$e/d = 12/32.7 = 0.367 < 0.70$; therefore, Fig. 4.2 should not be used.

From Fig. 4.9 for $\rho n = 0.05$, lower limit on $|e/d|$ should be read as 0.25. Because $0.367 > 0.25$, Fig. 4.4 and 4.5 should be used.

$$N/(bdE_c\alpha\Delta T) = 100{,}000/(12 \times 32.7 \times 4 \times 10^6 \times 5.5 \times 10^{-6} \times 80) = 0.145$$

For $N/(bdE_c\alpha\Delta T) = 0.145$ and $e/d = 0.367$, find $M_{\Delta T}$. By interpolation between e/ds:

$\rho n = 0.04$ (Fig. 4.4) at $e/d = 0.367$; 0.035 by interpolation

$\rho n = 0.06$ (Fig. 4.5) at $e/d = 0.367$; 0.046 by interpolation

For $\rho n = 0.05$, $(1 - \nu)M_{\Delta T}/bd^2E_c\alpha\Delta T = 1/2(0.035 + 0.046) = 0.0405$

$M_{\Delta T} = 0.0405(1.25)(12)(32.7)^2(4)(5.5)(80) = 1{,}143{,}000$ in.-lb

$M_{\Delta T} = 95.3$ ft-kips

Concrete and reinforcement stresses are calculated from a cracked section investigation with $N = 100$ kips compression and $M = 195.3$ ft-kips at section centerline.

4.4.4 ***Example 4:*** *Tensile* N *and* |e/d| < *0.70*

Same as Example 3, except $N = 60$ kips tension.

$e = 100$ ft-kips/(–60 kips) $= –1.67$ ft $= –20$ in., $e/d = –20/32.7 = –0.612$ or $|e/d| = 0.612$

From Fig. 4.9 for $\rho n = 0.05$, the lower limit on $|e/d|$ is 0.575 for the tensile N case. Because $0.612 > 0.575$, Fig. 4.2 should be used.

From Fig. 4.2, with $\rho n = 0.05$, read $(1 - \nu)M_{\Delta T}/(bd^2E_c\alpha\Delta T) = 0.032$

$M_{\Delta T} = 0.032(1.25)(12)(32.7)^2(4)(5.5)(80) = 75.3$ ft-kips

$M_{\Delta T} = 75.3$ ft-kips

Concrete and reinforcement stresses are calculated from a cracked section investigation with $N = 60$ kips tension and $M = 175.3$ ft-kips at section centerline.

4.4.5 *Summary of results for Examples 1, 2, 3, and 4*

A summary of results for Examples 1, 2, 3, and 4 can be found in Table 4.1.

CHAPTER 5—REFERENCES

5.1—Referenced standards and reports

The standards and reports listed below were the latest editions at the time this document was prepared. Because these documents are revised frequently, the reader is advised to contact the proper sponsoring group if it is desired to refer to the latest version.

American Concrete Institute

207.2R Effect of Restraint, Volume Change, and Reinforcement on Cracking of Mass Concrete

209R Prediction of Creep, Shrinkage, and Temperature Effects in Concrete Structures

318 Building Code Requirements for Structural Concrete

349 Code Requirements for Nuclear Safety-Related Concrete Structures

435.7R Report on Temperature-Induced Deflections of Reinforced Concrete Members

The above publications may be obtained from the following organization:

American Concrete Institute
PO Box 9094
Farmington Hills, MI 48333-9094
www.concrete.org

5.2—Cited references

ACI Committee 340, 1997, *ACI Design Handbook*, SP-17(97), American Concrete Institute, Farmington Hills, Mich., 482 pp.

ACI Committee 349, 2006, "Code Requirements for Nuclear Safety-Related Concrete Structures (ACI 349-06) and Commentary," American Concrete Institute, Farmington Hills, Mich., 149 pp.

Ferguson, P. M., 1965, *Reinforced Concrete Fundamentals*, 2nd Edition, John Wiley & Sons, Inc.

Fu, C. C., and Daye, M. D., eds., 1991, *Computer Analysis of Effects of Creep, Shrinkage, and Temperature Changes on Concrete Structures*, SP-129, American Concrete Institute, Farmington Hills, Mich., 191 pp.

Gurfinkel, G., 1972, "Thermal Effects in Walls of Nuclear Containment-Elastic and Inelastic Behavior," *Proceedings*, First International Conference on Structural Mechanics in Reactor Technology (Berlin, 1971), V. 5-J, Commission of the European Communities, Brussels, pp. 277-297.

Kohli, T., and Gurbuz, O., 1976, "Optimum Design of Reinforced Concrete for Nuclear Containments, Including Thermal Effects," *Proceedings*, Second ASCE Specialty Conference on Structural Design of Nuclear Plant Facilities (New Orleans, 1975), V. 1-B, American Society of Civil Engineers, New York, 1976, pp. 1292-1319.

Office of the Federal Register, 2002, "Quality Assurance Program Requirements for Nuclear Power Plants," Title 10 of the *Code of Federal Regulations*, Part 50, Appendix B.

APPENDIX A—EXAMPLES IN METRIC

A.1—Frame design example from 3.5

The continuous frame shown in Fig. A.1 is given with all components 305 mm wide x 610 mm thick and 75 mm cover on the reinforcement. The load combination to be considered is $U = D + L + T_o + E_{ss}$.

The mechanical loading consists of

$$W_D = 5.9 \text{ kN/m}$$

$$W_L = 9.9 \text{ kN/m}$$

on component *BC*, and a lateral load of 17 kN at joint *C* due to E_{ss}.

The thermal gradient T_o results from 54 °C interior and 10 °C exterior temperature. Thus, $T_m = (54 + 10)/2 = 32$ °C. The base temperature T_b is taken as 21 °C. For this condition, $T_m - T_b = 32\ °C - 21\ °C = +11$ °C and $\Delta T = 44$ °C (hot interior, cold exterior).

The material properties are $f'_c = 21$ MPa and $E_c = 2.15 \times 10^4$ MPa, $f_y = 420$ MPa and $E_s = 2 \times 10^5$ MPa; and $\alpha = 9 \times 10^{-6}$ mm/mm/°C. Also, $n = E_s/E_c = 9.3$.

The reinforcement in the frame consists of two No. 25 bars at each face in all components. This results in $\rho = A_s/bd = (2 \times 510)/(305[610 - 75]) = 0.0063$ and $\rho n = 9.3(0.0063) = 0.059$. $\omega = \rho f_y/f'_c = 0.0063(420/21) = 0.126$; and $K_u = f'_c\,\omega(1 - 0.59\omega) = 21 \times 0.126(1 - 0.59 \times 0.126) = 2.4$. The section capacity is $M_u = \phi K_u F = (0.9)(2.4) \times (305)(535)^2/1000 = 189{,}000$ m-N.

Mechanical loads—An analysis of the uncracked frame results in the component moments (m-N) as follows. Moments acting counterclockwise on a component are denoted as positive. These values were obtained by moment distribution, and moments due to E_{ss} include the effect of frame sidesway.

	Moment (m-N)
AB:	–70,900
BA:	–103,000
BC:	+103,000
CB:	–62,400
CD:	+62,400
DC:	+10,200

These are shown in Fig. A.1.

The maximum mechanical load moment of 103,000 m-N is less than the section capacity of 189,000 m-N. Therefore, the frame is adequate for mechanical loads

Thermal effects ($\Delta T = 44$ °C and $T_m - T_b = 11$ °C)

The $\Delta T = 44$ °C having hot interior and cold exterior is expected to produce thermal stresses that are tensile on the exterior faces of all components. These stresses will add to the existing exterior face tensile stresses due to the mechanical loads. Hence, the L_T and a values are arrived at from the mechanical load moment diagram in Fig. A.1.

Component	End	L_T/L, m/m	a/L_T, m/m
AB	A	3.6/6.1 = 0.59	0
AB	B	0.59	1
BC	B	(1.6 + 1.0)/9.1 = 0.29	1.6/2.6 = 0.61
BC	C	0.29	1.0/2.6 = 0.39
CD	C	5.2/6.1 = 0.86	1
CD	D	0.86	0

All components are the end-cracked type. Figures 3.4 through 3.6 are used to obtain the coefficients k_s and CO, which are shown in Table A.1.

The expressions from Section 3.4 for fixed-end moment (FEM) are evaluated as

$$1.\ \Delta T \text{ FEM} = \frac{E_c \alpha \Delta T b t^2 k_s}{12} \frac{}{2}(1 - CO)$$

$$= \frac{(2.15 \times 10^4)(9 \times 10^{-6})(44)(305)(610)^2 k_s}{12} \frac{}{2}(1 - CO)$$

$$\Delta T \text{ FEM} = 81 k_s (1 - CO)/2 \text{ m-kN}$$

$$2.\ T_m - T_b \text{ FEM} = \frac{E_c I_g}{L^2}(\Delta)(k_s)(1 + CO)$$

$$= \frac{(2.15 \times 10^4)(305)(610)^3}{(6100)^2}(\Delta)(k_s)(1 + CO)$$

Table A.1—Cracked frame coefficients and thermal moments on components

Component	End	L_T/L	a/L_T	k_s	CO	K_y/L	DF	Thermal FEMs, m-kN			Distributed thermal moments,* m-kN	Distributed thermal moments and mechanical moments, m-kN
								ΔT-44 FEM	$T_m - T_b = 11$ FEM	Total FEM		
AB	A	0.59	0	3.40	0.41	0.17	1.0	+81.5	–6.5	+75.0	+48.8	–22.1
AB	B	0.59	1	2.00	0.70	0.10	0.56	–24.4	–4.6	–29.0	–54.1	–157
BC	B	0.29	0.61	2.40	0.43	0.08	0.44	+56.5	0	+56.5	+54.1	+157
BC	C	0.29	0.39	2.65	0.38	0.088	0.48	–66.7	0	–66.7	–50.2	–113
CD	C	0.86	1	1.90	0.57	0.095	0.52	+33.2	+5.0	+38.2	+50.2	+113
CD	D	0.86	0	2.39	0.47	0.120	1.0	–51.4	+5.9	–45.5	–45.0	–34.8

*Corrected for sidesway.
Notes: $DFi = (k_{si}E_iI_{gi}/L_i)/(\Sigma k_{si}E_iI_{gi}/L_i)$; symbols with component i are indicated with subscript i.

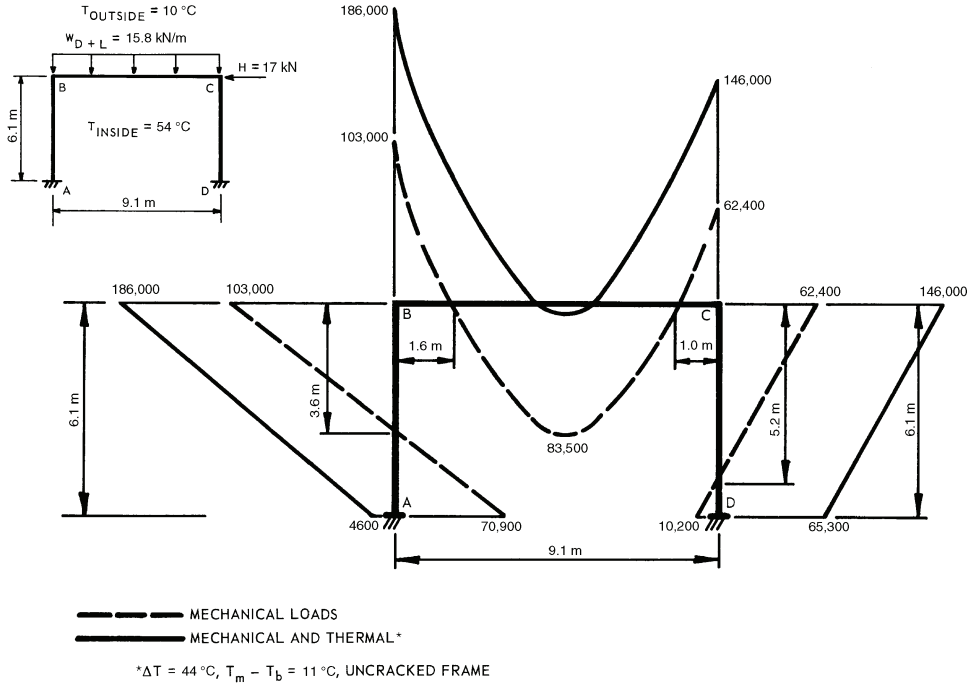

Fig. A.1—Uncracked moment frames (m-N).

$T_m - T_b$ FEM = $3.3(\Delta)(k_s)(1 - CO)$ m-kN

3. Δ = total unrestrained change of length of Component BC
= $\alpha(T_m - T_b)L$

$\Delta = (9 \times 10^{-6})(11)(9100)$

$\Delta = 0.90$ mm

Distribute 0.90 mm to Ends B and C of Components AB and CD, respectively, in inverse proportion to the shear stiffness at these ends.

Shear stiffness at B

$$= \frac{E_cI_g}{L^3}[k_{sA}(1 + CO_A) + k_{sB}(1 + CO_B)]$$

$$= \frac{E_cI_g}{L^3}[3.4(1.41) + 2.00(1.70)]$$

$$= \frac{E_cI_g}{L^3}(8.19)$$

Shear stiffness at C

$$= \frac{E_cI_g}{L^3}[k_{sC}(1 + CO_C) + k_{sD}(1 + CO_D)]$$

$$= \frac{E_cI_g}{L^3}[1.90(1.57) + 2.38(1.47)]$$

$$= \frac{E_cI_g}{L^3}(6.48)$$

Sum of shear stiffness at B and C = $\frac{E_cI_g}{L^3}(14.67)$

$\Delta_B = 0.90$ mm $(6.48/14.67) = 0.90 \times 0.44 = 0.40$ mm
$\Delta_C = 0.90$ mm $(8.19/14.67) = 0.90 \times 0.56 = 0.50$ mm

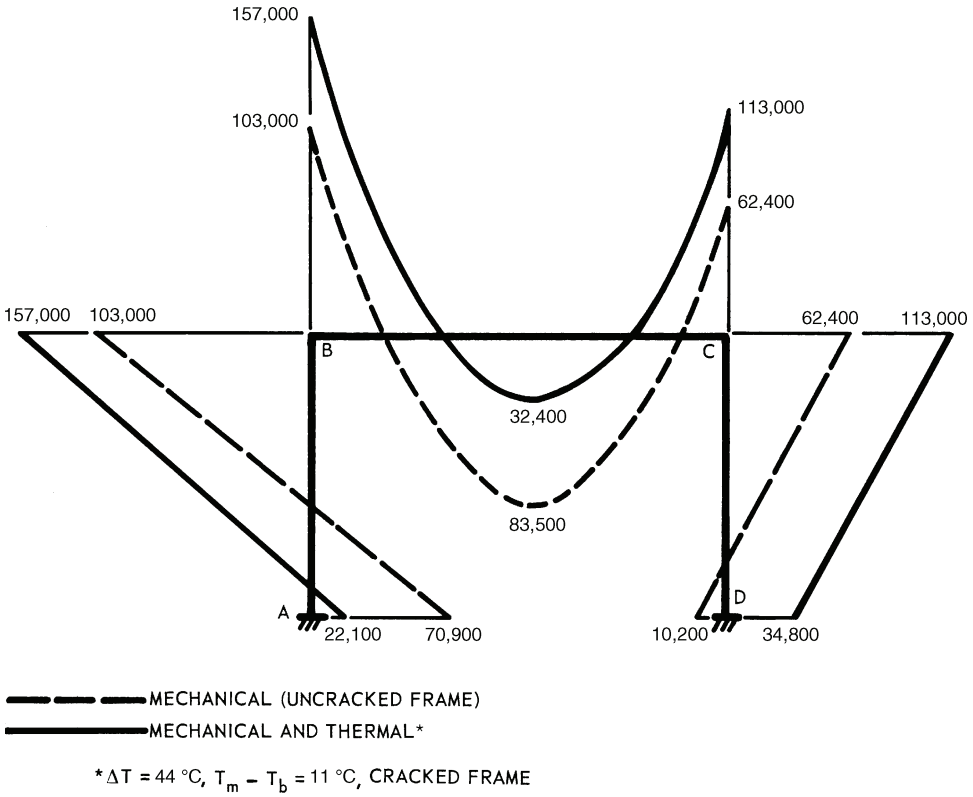

Fig. A.2—Final frame moment (m-N).

To demonstrate the effect of cracking on the thermal moments, the fixed-end thermal moments for the uncracked frame are obtained from the final expressions in 1 and 2 using $k_s = 4$, $CO = 1/2$, and $\Delta = (1/2)\alpha(T_m - T_b)L$, with L being the length of Component BC. A moment distribution is performed, and the resulting distributed moments are added to the mechanical moments. The combined moments are shown in Fig. A.1 for comparison with the cracked frame moments.

The fixed-end thermal moments for the cracked frame are obtained using the aforementioned values for Δ_B and Δ_C and by referring to Table A.1 for k_s and CO. These fixed-end moments and the resulting distributed thermal moments are given in Table. A.1. The distributed thermal moments include the effect of sidesway, which occurs because the frame in unsymmetrically cracked.

Combined loads—The final frame moments are shown in Table A.1 and Fig. A.2. These can be compared with Fig. A.1 to see the effect of the cracking reduction of thermal moments.

Although not shown, the component axial forces were evaluated to confirm that section cracking still corresponds to the pure bending condition of Assumption 3. Recall that e/d should be at least 0.5 for this condition. For Components AB and CD, the axial forces result primarily from the mechanical loads and are compressive. For Component BC, the axial force is compressive and includes the compression due to the 11 ºC increase on the component.

A.2—Design examples from 4.4

A.2.1 ***Example 1:*** *Compressive* N *and* |e/d| > 0.70, $\rho' = \rho$

$b = 305$ mm, $t = 914$ mm, $d = 831$ mm, $d' = 84$ mm, $A_s' = 1290$ mm^2, $A_s = 1935$ mm^2, $E_s = 200{,}000$ MPa, $E_c = 27{,}600$ MPa, $\nu = 0.2$, $N = 222{,}000$ N compression, $M = 136 \times 10^6$ mm-N, $\Delta T = 44$ °C

$n = E_s/E_c = 200/27.6 = 7.25$, $e = M/N = 1.36 \times 10^8/2.22 \times 10^5 = 610$ mm, $\rho' = 1290/(305 \times 914) = 0.0046$, $\rho' n = 0.0046 \times 7.25 = 0.033$, $\rho = 1935/(305 \times 914) = 0.0069$, $\rho n = 0.0069 \times 7.25 = 0.050$

Cracked thermal moment $M_{\Delta T}$

e/d ratio: $e/d = 610/831 = 0.73 > 0.70$; therefore, Section 4.2 results should be used.

Because $t/d = 1.1$ and $d'/d = 0.10$, Fig. 4.2 should be used. Because $\rho' \neq \rho$, however, interpolate between the two curves.

From Fig. 4.2 for $\rho n = 0.050$, $(1 - \nu)M_{\Delta T}/(bd^2E_c\alpha\Delta T)$ should be read as

$$0.0303 \text{ for } \rho' = 0$$

$$0.0320 \text{ for } \rho' = \rho$$

Interpolate for $\rho' = 0.0046$

$$(1 - \nu)M_{\Delta T}/(bd^2E_c\alpha\Delta T) = 0.0303 + (0.0320 - 0.0303)(0.0045/0.0069) = 0.0314$$

$$(1 - \nu)M_{\Delta T} = [0.0314(305)(831)^2(27{,}600) \times (9.9 \times 10^{-6})(44)]/1000 = 79.5 \times 10^6 \text{ mm-N}$$

Table A.2—Summary of results for Examples 1, 2, 3, and 4

Example	Axial force N, kN	Type	Moment M, m-kN	Temperature differential ΔT, °C	Compression reinforcement A_s', mm^2	Tension reinforcement A_s, mm^2	Cracked thermal moment $M_{\Delta T}$, m-kN	Total moment $(M + M_{\Delta T})$, m-kN	e/d	Use figure
1	222	Compression	136	44	1290	1935	99.4	236	0.733 > 0.70	Use Fig. 4.2
2	222	Tension	136	44	1935	1935	101	238	0.733 > 0.70	Use Fig. 4.2
3	445	Compression	136	44	1935	1935	128	265	0.37 < 0.70 0.37 > 0.25	Use Fig. 4.4, 4.5, and 4.9
4	267	Tension	136	44	1935	1935	101	238	0.612 < 0.70 0.612 > 0.575	Use Fig. 4.2 and 4.9

$M_{\Delta T} = 99.4 \times 10^6$ mm-N or 99.4 m-kN

Check using equations

$$k_{N=0} = \sqrt{(2\rho' n + \rho n)^2 + 2[2\rho' n(d'/d) + \rho n]}$$

$$- (2\rho' n + \rho n) = [(2 \times 0.033 + 0.050)^2 + 2(2 \times 0.033 \times 0.10 + 0.050)]^{1/2} - (2 \times 0.033 + 0.050) = 0.239$$

$$(1 - \nu)M_{\Delta T}/(bd^2E_c\alpha\Delta T) = -0.152k^3 + 1.818\rho' n(d'/d - k) \times (d'/d) + 0.909\rho n(1 - k) = -0.152(0.239)^3 + 1.818(0.034) \times (0.1 - 0.239)(0.10) + 0.909(0.050) \times (1 - 0.239) = 0.0317$$

$M_{\Delta T} = 99.4$ m-kN$(0.0317/0.0314) = 100$ m-kN ≈ 99.4 m-kN, OK

Concrete and reinforcement stresses are calculated from a cracked section investigation with $N = 222$ kN compression and $M = 236$ m-kN at section centerline.

A.2.2 ***Example 2:*** *Tensile* N *and* |e/d| > *0.70*, $\rho' = \rho$

$b = 305$ mm, $t = 914$ mm, $d = 831$ mm, $d' = 84$ mm, $A_s' = A_s = 1935$ mm^2, $E_s = 200{,}000$ MPa, $E_c = 27{,}600$ MPa, $\nu = 0.2$, $N = 222{,}000$ N tension, $M = 136 \times 10^6$ mm-N, and $\Delta T = 44$ °C

$n = 7.25$, $e = 1.36 \times 10^8/-2.22 \times 10^5 = -610$ mm, $\rho' = \rho = 0.0069$, $\rho' n = \rho n = 0.050$

Cracked thermal moment $M_{\Delta T}$

$e/d = -610/831 = -0.73$, $|e/d| = 0.73 > 0.7$; therefore, Fig. 4.2 should be used.

From Fig. 4.2 with $\rho' n = 0.050$ and $\rho' = \rho$ curve,

$$(1 - \nu)M_{\Delta T}/(bd^2E_c\alpha\Delta T) = 0.032$$

$M_{\Delta T} = (1.25)(305)(831)^2(27{,}600)(9.9 \times 10^{-6})(44)(0.032) = 101 \times 10^6$ mm-N or 101 m-kN.

Concrete and reinforcement stresses are calculated from a cracked section investigation with $N = 222$ kN tension and $M = 238$ m-kN at section centerline.

A.2.3 ***Example 3:*** *Compressive* N *and* |e/d| < 0.70

Same section as Example 2.

$N = 445{,}000$ N compression, $M = 136 \times 10^6$ mm-N, $\Delta T = 44$ °C,

$$e = \frac{136{,}000{,}000 \text{ mm-N}}{445{,}000 \text{ N}} = 305 \text{ mm}$$

$e/d = 305/831 = 0.37 < 0.70$; therefore, Fig. 4.2 should not be used.

From Fig. 4.9 for $\rho n = 0.05$, lower limit on $|e/d|$ should be read as 0.25. Because $0.37 > 0.25$, Fig. 4.4 and 4.5 should be used.

$$N/(bdE_c\alpha\Delta T) = 445{,}000/(305 \times 831 \times 27{,}600 \times 9.9 \times 10^6 \times 44) = 0.145$$

For $N/(bdE_c\alpha\Delta T) = 0.145$ and $e/d = 0.37$, find $M_{\Delta T}$. By interpolation between e/ds:

$\rho n = 0.04$ (Fig. 4.4) at $e/d = 0.37$; 0.035 by interpolation

$\rho n = 0.06$ (Fig. 4.5) at $e/d = 0.37$; 0.046 by interpolation

For $\rho n = 0.05$, $(1 - \nu)M_{\Delta T}/bd^2E_c\alpha\Delta T = 1/2(0.035 + 0.046) = 0.0405$

$M_{\Delta T} = 0.0405(1.25)(305)(831)^2(27{,}600)(9.9 \times 10^{-6})(44) = 128 \times 10^6$ mm-N or 128 m-kN

Concrete and reinforcement stress are calculated from a cracked section investigation with $N = 445$ kN compression and $M = 265$ m-kN at section centerline.

A.2.4 ***Example 4:*** *Tensile* N *and* |e/d| < *0.70*

Same as Example 3, except $N = 267{,}000$ N tension.

$e = 136 \times 10^6$ mm-N/(–267,000 N) = –509 mm, $e/d = -509/831 = -0.612$ or $|e/d| = 0.612$

From Fig. 4.9 for $\rho n = 0.05$, the lower limit on $|e/d|$ is 0.575 for the tensile N case. Because $0.612 > 0.575$, Fig. 4.2 should be used.

From Fig. 4.2, with $\rho n = 0.05$, read $(1 - \nu)M_{\Delta T}/(bd^2E_c\alpha\Delta T) = 0.032$

$M_{\Delta T} = 0.032(1.25)(305)(831)^2(27{,}600)(9.9 \times 10^{-6})(44) = 101 \times 10^6$ mm-N or 101 m-kN

Concrete and reinforcement stresses are calculated from a cracked section investigation with $N = 276$ kN tension and $M = 238$ m-kN at section centerline.

A.2.5 *Summary of results for Examples 1,2, 3, and 4*

Table A.2 shows the summary of results for Examples 1, 2, 3, and 4.

American Concrete Institute®
Advancing concrete knowledge

As ACI begins its second century of advancing concrete knowledge, its original chartered purpose remains "to provide a comradeship in finding the best ways to do concrete work of all kinds and in spreading knowledge." In keeping with this purpose, ACI supports the following activities:

- Technical committees that produce consensus reports, guides, specifications, and codes.
- Spring and fall conventions to facilitate the work of its committees.
- Educational seminars that disseminate reliable information on concrete.
- Certification programs for personnel employed within the concrete industry.
- Student programs such as scholarships, internships, and competitions.
- Sponsoring and co-sponsoring international conferences and symposia.
- Formal coordination with several international concrete related societies.
- Periodicals: the *ACI Structural Journal* and the *ACI Materials Journal*, and *Concrete International*.

Benefits of membership include a subscription to *Concrete International* and to an ACI Journal. ACI members receive discounts of up to 40% on all ACI products and services, including documents, seminars and convention registration fees.

As a member of ACI, you join thousands of practitioners and professionals worldwide who share a commitment to maintain the highest industry standards for concrete technology, construction, and practices. In addition, ACI chapters provide opportunities for interaction of professionals and practitioners at a local level.

American Concrete Institute
38800 Country Club Drive
Farmington Hills, MI 48331
U.S.A.
Phone: 248-848-3700
Fax: 248-848-3701

www.concrete.org

Reinforced Concrete Design for Thermal Effects on Nuclear Power Plant Structures

The AMERICAN CONCRETE INSTITUTE

was founded in 1904 as a nonprofit membership organization dedicated to public service and representing the user interest in the field of concrete. ACI gathers and distributes information on the improvement of design, construction and maintenance of concrete products and structures. The work of ACI is conducted by individual ACI members and through volunteer committees composed of both members and non-members.

The committees, as well as ACI as a whole, operate under a consensus format, which assures all participants the right to have their views considered. Committee activities include the development of building codes and specifications; analysis of research and development results; presentation of construction and repair techniques; and education.

Individuals interested in the activities of ACI are encouraged to become a member. There are no educational or employment requirements. ACI's membership is composed of engineers, architects, scientists, contractors, educators, and representatives from a variety of companies and organizations.

Members are encouraged to participate in committee activities that relate to their specific areas of interest. For more information, contact ACI.

www.concrete.org

American Concrete Institute®
Advancing concrete knowledge